Thymidylate Synthase O-GlcNAcylation: a molecular mechanism of 5-FU sensitization in colorectal cancer

Ninon Very, Stéphan Hardivillé, Amélie Decourcelle, Julien Thévenet, Madjid Djouina, Adeline Page, Gérard Vergoten, Céline Schulz, Julie Kerr-Conte, Tony Lefebvre, et al.

Thymidylate Synthase *O*-GlcNAcylation: a molecular mechanism of 5-FU sensitization in colorectal cancer

Ninon Very[1], Stéphan Hardivillé[1], Amélie Decourcelle[2], Julien Thévenet[3], Madjid Djouina[4], Adeline Page[5], Gérard Vergoten[4], Céline Schulz[1], Julie Kerr-Conte[3], Tony Lefebvre[1], Vanessa Dehennaut[2] and Ikram El Yazidi-Belkoura[1*].

[1] Université de Lille, CNRS, UMR8576 - UGSF - Unité de Glycobiologie Structurale et Fonctionnelle, F-59000, Lille, France.

[2] Université de Lille, CNRS, INSERM, CHU Lille, UMR9020-U1277 - CANTHER - Cancer Heterogeneity Plasticity and Resistance to Therapies, F-59000, Lille, France.

[3] Université de Lille, Inserm, CHU Lille, Institut Pasteur Lille, U1190 - EGID, F-59000 Lille, France.

[4] Université de Lille, Inserm, CHU Lille, U1286 - INFINITE - Institute for Translational Research In Inflammation, F-59000 Lille, France.

[5] Protein Science Facility, SFR BioSciences, CNRS UMS3444, INSERM US8, UCBL, ENS de Lyon, 69007 Lyon, France.

**** Correspondence*** to **Ikram El Yazidi-Belkoura at** ikram.el-yazidi@univ-lille.fr

The authors declare no potential conflicts of interest.

Abstract

Alteration of *O*-GlcNAcylation, a dynamic post-translational modification, is associated with tumorigenesis and tumor progression. Its role in chemotherapy response is poorly investigated. Standard treatment for colorectal cancer (CRC), 5-fluorouracil (5-FU), mainly targets Thymidylate Synthase (TS). TS *O*-GlcNAcylation was reported but not investigated yet. We hypothesize that *O*-GlcNAcylation interferes with 5-FU CRC sensitivity by regulating TS. *In vivo*, we observed that combined 5-FU with Thiamet-G (*O*-GlcNAcase (OGA) inhibitor) treatment had a synergistic inhibitory effect on grade and tumor progression. 5-FU decreased *O*-GlcNAcylation and, reciprocally, elevation of *O*-GlcNAcylation was associated with TS increase. *In vitro* in non-cancerous and cancerous colon cells, we showed that 5-FU impacts *O*-GlcNAcylation by decreasing *O*-GlcNAc Transferase (OGT) expression both at mRNA and protein levels. Reciprocally, *OGT* knockdown decreased 5-FU-induced cancer cell apoptosis by reducing TS protein level and activity. Mass spectrometry, mutagenesis and structural studies mapped *O*-GlcNAcylated sites on T251 and T306 residues and deciphered their role in TS proteasomal degradation. We reveal a crosstalk between *O*-GlcNAcylation and 5-FU metabolism *in vitro* and *in vivo* that converges to 5-FU CRC sensitization by stabilizing TS. Overall, our data propose that combining 5-FU-based chemotherapy with Thiamet-G could be a new way to enhance CRC response to 5-FU.

Introduction

Thymidylate Synthase (TS) is a key ubiquitous enzyme involved in the *de novo* biosynthesis of 2'-deoxythymidine-5'-monophosphate (dTMP) and dihydrofolate (DHF) from 2'-dexoyuridine-5'-monophosphate (dUMP) and 5,10-methylenetetrahydrofolate (5,10-MTHF). dTMP is an essential precursor for DNA synthesis and repair. TS expression and activity are increased in cancer to support high cell proliferation rate, hence its inhibition is used in therapeutic strategies of several cancers including colorectal cancer (CRC) (1,2). 5-fluorouracil (5-FU) is the gold standard treatment for CRC. In cells, 5-FU is converted into the active metabolite 5-fluoro-2'-deoxyuridine monophosphate (FdUMP) which forms an

inactive complex with TS and 5,10-MTHF. This irreversible inhibition induces an accumulation of dUTP and a depletion of 2'-deoxythymidine-5'-triphosphate (dTTP) leading to DNA damage and cell cycle arrest. Resistance to 5-FU chemotherapy remains a challenge in the management of CRC and clinical outcome remains poor in patients with advanced cancers. High TS expression levels and single nucleotide polymorphism in TS gene (*TYMS*) are clinical predictive biomarkers of 5-FU-based chemotherapy resistance in CRC. However, numerous clinical studies on *TYMS* expression and polymorphism in human cancers to clarify its significance as a determinant of tumors 5-FU sensitivity do not appear consistent due to the variability in the genetic backgrounds of the patients (3,4). Adequate amount of TS appears to be necessary for 5-FU sensitivity. Post-translational modifications (PTMs) regulate enzymatic activity, nuclear translocation and degradation of TS. TS is phosphorylated (5,6), SUMOylated (7), N^{α}-acetylated (8), ubiquitinated (8) and *O*-GlcNAcylated (9,10). However, the role of these PTMs in the 5-FU response remains unknown. *O*-GlcNAcylation is a dynamic PTM finely tuned by two antagonistic enzymes: *O*-GlcNAc transferase (OGT) and *O*-GlcNAcase (OGA) that respectively transfers and hydrolyzes the *O*-GlcNAc moiety on serine and threonine residues of proteins in response to cell nutrient state. This PTM regulates interactions, stability, enzymatic activity and subcellular localization of target proteins, hence a plethora of fundamental cellular mechanisms (11). Alteration of *O*-GlcNAcylation was reported in many cancers and several studies pointed out its involvement in the etiology and progression of the disease (12). Emerging research demonstrates that *O*-GlcNAcylation could also regulate the response of cancerous cells to therapeutic drugs such as tamoxifen (13), Tumor necrosis factor related apoptosis-Inducing ligand (TRAIL) therapy (14,15), cisplatin (16–18), bortezomib (19,20), doxorubicin (21) and 5-FU (22). Herein, we report multiple lines of *in vivo* and *in vitro* data supporting the *O*-GlcNAcylation sensitizing effect to 5-FU response in CRC, involving the novel finding that this PTM at Thr^{251} and Thr^{306} stabilizes TS.

Materials and Methods

Cell lines

CCD 841 CoN (CRL-1790) and parental HT-29 (HTB-38), purchased from American Type Culture Collection (ATCC), and 5-FU resistant HT-29 5F31 cells (23) were cultured respectively in EMEM with 5 mM glucose, McCoy's 5A and DMEM with 25 mM glucose (Lonza) supplemented with 10% heat inactivated FBS (Dutscher) and 2 mM L-glutamine. Cells were seeded or transfected in their respective medium and then, 24 h later, grown in DMEM with 25 mM glucose (High Glucose, HG) unless stated otherwise in figure legend. For transfection procedures see supplemental material.

Animal models

Animal care and procedures were carried out according to the French guidelines (APAFIS#1879-2018121918307521) by the Ethics Committee on Animal Experiments (CEEA) 75 Hauts-de-France. Forty-five C57BL/6J OlaHsd wild-type age-matched (8 weeks) male mice (Envigo Harlan) were housed in groups of 10 per cage using a 12 h light/12 h dark cycle and provided with water and standard diet (SAFE) *ab libitum.* Forty mice were injected intraperitoneally with 10 mg/kg AOM (Sigma-Aldrich) and 5 mice received an injection of a vehicle (NaCl 0.9%) (untreated, healthy controls). The AOM-injected mice were given 3 cycles of DSS (MP Biomedicals™) as follow: DSS 2.5% for 7 days in week 1, DSS 1.5% for 5 days in week 3 and DSS 1.5% for 5 days in week 8. CRC induction was monitored under anesthesia and colonoscopies were performed at day 68 using a high-resolution Karl Storz colonoscope (Tuttlingen). At day 73, AOM-injected and control mice were randomized in 4 groups: vehicle (NaCl 0.9%), 5-FU (12.5 mg/kg/day) (Sigma-Aldrich), Thiamet-G (90 mg/kg/day) and 5-FU + Thiamet-G. ALZET® osmotic pumps were subcutaneously implanted under anesthesia with a connected ALZET® intraperitoneal catheter (Charles River) for continuous drug delivery at 0.5 µL/h for 13 days. At day 86, tumor numbers and grade were assessed by colonoscopy (24). After sacrifice, colons were dissected, flash-frozen and stored at -80°C or fixed in 10% buffered formalin for paraffin embedment.

Plasmids

See **Supplemental Experimental Procedures and Supplemental Table S1**.

Cell growth assay and IC_{50} determination

Cells were seeded in a 96-well microplate 24 h prior treatment with increasing concentrations of 5-FU (0 to 20 µM for CCD 841 CoN and HT-29 cells, 0 to 50 mM for HT-29 5F31) for 48 h. Cell viability was analyzed using CellTiter 96® AQueous One Solution Cell Proliferation Assay (Promega) following the manufacturer's instructions. Analysis of siOGT effect on the 5-FU IC_{50} value was monitored on 24 h siOGT or siControl transfected cells that were then incubated 72 h with a range of 5-FU (0 to 80 µM for CCD 841 CoN and HT-29 cells, 0 to 50 mM for HT-29 5F31). The cell viability was assessed in the same way.

Cell cycle analysis

Cells were harvested using trypsin/EDTA, washed twice with Phosphate-buffered saline (PBS) and fixed. Cells were then washed twice with PBS and incubated for 1 h at 37°C with 10 ng/mL RNAse A (Sigma-Aldrich) and 500 µg/mL propidium iodide (Sigma-Aldrich). DNA content was analyzed using FACScalibur cytometer (BD Biosciences).

SDS-PAGE and Western Blot

See **Supplemental Experimental Procedures**.

Immunoprecipitation and co-immunoprecipitation

See **Supplemental Experimental Procedures**.

Click chemistry

Two-hundred micrograms of total proteins was methanol/chloroform precipitated and subjected to Click-It™ *O*-GlcNAc Enzymatic Labelling System (Thermo Fisher Scientific) following the manufacturer's

instructions. GalNAz labeled samples (50 µg) were chemically labeled with 10 mM homemade DBCO-PEG mass tag (4.4 kDa) as previously described (25).

Real time RT-qPCR

See **Supplemental Experimental Procedures and Supplemental Table S1**.

Mass spectrometry

Following SDS-PAGE of immunopurified TS and Coomassie Brilliant Blue staining, the TS was in-gel digested with trypsin, and released peptides were analyzed by high resolution mass spectrometry according to a previously published protocol (25) and further details in **Supplemental Experimental Procedures**.

TS activity

TS activity assay was measured according to the tritium-release assay (26) after cytosol incubation with 0.375 µCi [5-^{3}H]-dUMP (Isobio) and 0.62 mM CH_2FH_4 (Santa Cruz). Radiolabeled $^{3}H_2O$ was measured by Ultima Gold^{TM} liquid scintillation (PerkinElmer) with a Hidex 300 SL scintillation counter. Cellular and intrinsic activity of TS were respectively normalized using total proteins and TS proteins levels.

Immunohistochemistry

Immunohistochemistry staining and quantification on formalin fixed colon tissues were realized as we previously described (27). Antigen retrieval on deparaffinized and rehydrated 4 µm histological sections was performed in Tris-HCl 10 mM, EDTA 1 mM, pH 9 for anti-TS antibody [EPR4545] or Tris sodium citrate 10 mM pH 6 for anti-*O*-GlcNAc antibody. The rabbit anti-TS [EPR4545] (1:100) or the anti-*O*-GlcNAc (1:1,000) antibody were incubated overnight at 4°C.

***In silico* modeling of TS structure**

Tridimensional structures of the human TS were retrieved from the Protein Data Bank (www.rcsb.org) under the PDB codes 1HZW (X-ray diffraction at 2.0 angstroms resolution) and 1I00 (X-ray diffraction at 2.5 angstroms resolution) (28). Missing sequences M1-G29 and I307-V313 were built and added to the X-ray structure 1HZW. A conformational analysis of the whole structure was performed keeping the E30-T306 as aggregate. Once the amino acids under study were modified, they were optimized within the protein using a classical Monte Carlo conformational searching procedure as described in the BOSS software (29). An empirical potential energy was further evaluated for the various post-translationally modified TS using the SPASIBA force field and the corresponding parameters, in particular for proteins and saccharides (30,31). Stabilization energies of modified TS relative to unmodified TS were given. Molecular graphics and analysis were performed using BIOVIA Discovery Studio Visualizer (Dassault Systèmes, 2020).

Statistical analyses

All experiments are at least 3 independent replicates unless stated otherwise. Statistical analyses were performed with Prism 8. Further details are in **Supplemental Experimental Procedures.**

Data availability

Microarray GSE104645 data are available in the Gene Expression Omnibus (GEO) repository, https://www.ncbi.nlm.nih.gov/geo/geo2r/?acc=GSE104645.

Results

O-GlcNAcylation potentiates CRC sensitivity to 5-FU chemotherapy *in vivo*

To investigate the effect of *O*-GlcNAcylation on CRC progression and response to 5-FU *in vivo*, we induced CRC in C57BL/6J OlaHsd mice using azoxymethane (AOM)/ Dextran Sulfate Sodium (DSS) combination **(Supplemental Fig. S1a)** that was shown to mimic a wide variety of tumors of all CRC consensus molecular subgroups (32). The induction of tumors was checked by colonoscopy 10 weeks after AOM injection

(**Supplemental Fig. S1a and b**). Vehicle, 5-FU and/or Thiamet-G, a pharmacological inhibitor of OGA, was then delivered continuously for 13 days. Before sacrifice, tumor number and grade were analyzed and scored by colonoscopy. Consistent with the literature, immunoblotting and immunohistochemistry showed hyper-*O*-GlcNAcylation of proteins in CRC tumors (+AOM) compared to healthy tissues without affecting OGT levels **(Supplemental Fig. S1c and d)**. An elevated *O*-GlcNAcylation level was accompanied by an increase in TS amount **(Supplemental Fig. S1c and d)**. In AOM/DSS treated mice, in comparison to control treatment, tumor number was reduced upon Thiamet-G or 5-FU treatment, and in mice that received both drugs **(Fig. 1a and b)**. All treatments reduced low-grade 1 tumors but only combined treatment reduced those of high-grade 4 and 5 tumors **(Fig. 1c)**. Thiamet-G and 5-FU alone or in combination decreased the percentage of mice with grade 5 tumors and increased those with grade 3 and 4 **(Fig.1d)**. The percentage of grade 3 tumors was higher in co-treatment condition than in Thiamet-G or 5-FU treatment alone, suggesting that the combination of 5-FU and Thiamet-G further delays the progression of the disease. In AOM/DSS treated mice, Thiamet-G treatment triggered an increase of global *O*-GlcNAcylation in CRC tumors which was associated with a decrease in OGT levels **(Fig. 1e)** suggesting a compensatory mechanism as previously reported (33)**.** Elevation of *O*-GlcNAcylation was also accompanied with a trend of increased TS levels **(Fig. 1e and f)**. As expected (34), we observed the heavy TS isoform (38 kDa) complexed with 5,10-MTHF and FdUMP confirming 5-FU incorporating into CRC tissue **(Fig. 1e)**. 5-FU treatment led to a decrease of global *O*-GlcNAcylation without affecting OGT levels **(Fig. 1e)**. Interestingly, Thiamet-G induced increase in *O*-GlcNAcylation returned close to control levels upon 5-FU co-treatment in CRC tumors **(Fig. 1e)** and more precisely in the epithelium **(Fig. 1f)**. TS levels were further increased in co-treatment condition compared to the 5-FU condition alone **(Fig. 1e and f)**. Thus, *in vivo* data suggest a crosstalk between *O*-GlcNAcylation and 5-FU metabolism, and a sensitizing effect of *O*-GlcNAcylation to 5-FU cytotoxicity possibly by increasing TS protein levels. Finally, we examined the relevance of this data in the human physiopathology from the microarray dataset GSE104645. We analyzed the *OGT* and *TYMS* mRNA expression profiles from primary non-treated tumors of metastatic CRC patients subsequently treated with first line 5-FU-based chemotherapy **(Fig. 1g and Supplemental Table S2)**.

Interestingly, while *TYMS* expression was not correlated to chemotherapy response in this cohort, *OGT* mRNA level was significantly higher in responders compared to non-responder patients **(Fig. 1g)** suggesting that high expression of *OGT* and the consequent higher *O*-GlcNAcylation could modulate 5-FU sensitivity.

5-FU decreases cellular *O*-GlcNAcylation *in vitro*

To decipher the relationship between *O*-GlcNAcylation, TS and cellular response to 5-FU, we first compared OGT, *O*-GlcNAcylation and TS levels in CCD 841 CoN non-cancerous and cancerous cell lines. As expected, OGT, *O*-GlcNAcylation and TS levels were increased in cancer cells compared to non-cancerous ones **(Fig. 2a)**. While OGT and *O*-GlcNAcylated protein levels are similar between parental HT-29 and 5-FU resistant HT-29 5F-31 cells, TS level is 10-fold higher in HT-29 5F31 compared to HT-29 cells **(Fig. 2a)** due to amplification of *TYMS* gene (23). Also, and as expected, HT-29 5F31 showed an IC_{50} to 5-FU of three log higher than its HT29 counterpart and CCD 841 CoN **(Fig. 2b)**. CCD 841 CoN cells were less sensitive to S-phase dependent 5-FU cytotoxicity than HT-29 cells **(Supplemental Fig. S2a and b)** most likely due to their very low growth rate. Compared to parental HT-29 cells and as expected, HT-29 5F31 cells showed a strong resistance to 5-FU treatment (**Fig. 2b and Supplemental Fig. S2a and b**) probably due to high TS expression **(Fig. 2a)**. In all subsequent experiments, we treated both cell lines with the 5-FU clinical concentration used of 6 µM, which induced S-phase arrest within 24 h and apoptosis at 72 h in HT-29 cells **(Supplemental Fig. S2a and b)**. We next investigated the effect of 5-FU treatment on OGT and *O*-GlcNAcylation levels. Upon 24 h of treatment, 5-FU led to decreased protein *O*-GlcNAcylation **(Fig. 2c)** concurrent with a decrease of both OGT mRNA **(Fig. 2d)** and protein **(Fig. 2c)** levels in CCD 841 CoN and HT-29 cell lines while it had no effect on HT-29 5F31 cells. These results indicate that 5-FU affects *O*-GlcNAcylation by decreasing *OGT* at a transcriptional level in non-cancerous and cancerous colon cells but not in 5-FU resistant ones.

***O*-GlcNAcylation modulates sensitivity to 5-FU and TS activity in colon cancer cells**

We then wondered whether *O*-GlcNAcylation could impact sensitivity to 5-FU by regulating TS. SiRNA downregulation of *OGT* led to a decrease of protein *O*-GlcNAcylation and TS levels **(Fig. 3a)**. In CCD 841 CoN cells, *OGT* knockdown drastically reduced free TS level **(Fig. 3a)** and cellular activity **(Fig. 3b)** by approximately 75% in untreated cells but had no effect on 5-FU treated cells. 5-FU or *OGT* downregulation did not affect cell cycle progression of CCD 841 CoN cells **(Supplemental Fig. S3a)**. In HT-29 cells, siOGT treatment led to a drastic decrease of TS level **(Fig. 3a)** and cellular activity in control and 5-FU treatment conditions **(Fig. 3b)**. In all cell lines treated or not with 5-FU, *OGT* knockdown did not affect *TYMS* mRNA level **(Fig. 3c)** suggesting that the TS regulation would occur at protein level. SiOGT did not modulate either intrinsic TS activity **(Supplemental Fig. S3b)** nor TS subcellular localization **(data not shown)**. 5-FU treatment induced S-phase arrest and apoptosis of HT-29 cells as observed by the increase of sub-G_1 phase cell population **(Supplemental Fig. S3b)** and the PARP-1 cleavage **(Fig. 3a).** *OGT* knockdown in HT-29 cells led to an increase of the 5-FU IC_{50} compared to control condition (36.62 µM ± 1.68 *versus* 26.84 µM ± 1.22 respectively) **(Fig. 3d)** along with a reduction of apoptosis by more than 30% **(Fig. 3a and Supplemental Fig. S3b)**. These results suggest that reduced *O*-GlcNAcylation would counteract sensitivity to 5-FU possibly by decreasing TS amount. We then hypothesized that increasing TS levels would counteract siOGT effects on HT-29 5-FU sensitivity. Overexpression of 3xFLAG-TS **(Fig. 3e)** rendered HT-29 cells resistant to 5-FU **(Fig. 3f)**. SiOGT decreased both endogenous and 3xFLAG-TS levels confirming that *O*-GlcNAcylation regulates TS protein level in a transcription independent manner. Reduction of sensitivity to 5-FU induced by siOGT was counteracted by the overexpression of recombinant 3xFLAG-TS **(Fig. 3e and f).** In HT-29 5F31 cells overexpressing TS, siOGT did not affect neither levels nor intrinsic activity of TS as expected **(Fig. 3a and b)**. The cell cycle distribution of siOGT transfected HT-29 5F31 cells remained unchanged in presence of 5-FU **(Supplemental Fig. S3b)**. Together, our data showed that knockdown of *OGT* lowered cancer cell sensitivity to 5-FU by decreasing TS levels and consequently its cellular activity in non-cancerous and cancerous 5-FU sensitive cells but not in their resistant counterparts.

TS interacts with OGT and is *O*-GlcNAcylated

We next hypothesized that TS is regulated by *O*-GlcNAcylation and that GlcNAc precursors, glucose and glucosamine ($GlcNH_2$), regulate its levels. in HT-29 cells, *O*-GlcNAcylation levels are lowered or barely detectable under low glucose (LG, 5 mM) or no glucose (0G) conditions respectively **(Fig. 4a)**. The reduced *O*-GlcNAcylation levels could be restored by complementing 0G media with $GlcNH_2$ **(Fig. 4a)**. Conversely, high glucose media (HG, 25 mM) enhanced *O*-GlcNAcylation levels compared to LG condition **(Fig. 4a)**. TS levels were highly decreased under glucose deprivation, and were partially restored by $GlcNH_2$ treatment. More notably, reduced glucose levels and *OGT* knockdown led to a decrease in TS **(Fig. 4a)**. These results indicate that TS expression level is impacted by *O*-GlcNAcylation in a nutrient dependent manner. We then performed a set of experiments to get more insight on the *O*-GlcNAcylation of TS. Co-immunoprecipitation experiments in HT-29 5F31 cells that highly express TS **(Fig. 2a)** showed that OGT interacts with TS in both control and 5-FU treated cells **(Fig. 4b)**. Immunoblotting of immune purified TS from HT-29 cells lysate with a pan anti-*O*-GlcNAc antibody revealed a signal that was decreased by *OGT* silencing, showing the *O*-GlcNAc modification of the enzyme **(Fig. 4c)**. Interestingly, while siOGT decreased total TS proteins (input), it slightly affected *O*-GlcNAcylation of immunoprecipitated TS suggesting that this PTM is abundant and/or stable, and may have a major impact on TS protein levels. We then performed *O*-GlcNAc mass tag experiments using a 4.4 kDa PEG to monitor TS *O*-GlcNAc stoichiometry in CCD 841 CoN and HT-29 cells. In both cell lines, we observed a PEGylated-*O*-GlcNAc-TS isoform with an apparent molecular weight shift of + 4-5 kDa showing that TS is the recipient of one *O*-GlcNAcylation **(Fig. 4d)**. In HT-29 cells, a second PEGylated-*O*-GlcNAc-TS isoform bearing 4 *O*-GlcNAc was also detected as shown by an apparent molecular weight shift of + 17-18 kDa. Interestingly, PEG-*O*-GlcNAc-TS underwent an extra shift upon 5-FU treatment revealing that the complexed TS isoform is also *O*-GlcNAcylated in both cell lines. We also noted that TS *O*-GlcNAcylation levels were higher in cancer cells (27% of total TS) compared to non-cancerous cells (9%) and that 5-FU did not significantly affect the TS *O*-GlcNAc stoichiometry **(Fig. 4d)**. We next mapped TS PTMs by HCD-MS/MS in HT-29 and HT-29 5F31 cells treated with Thiamet-G to stabilize *O*-GlcNAcylation. We identified an *O*-GlcNAcylated peptide covering the T234, T241 and T251 **(Fig. 4e)**. We precised the *O*-GlcNAc position at the T251 residue and its role on TS

stabilization by transfection of the three single threonine mutated TS-FLAG (**Supplemental Fig S4**). Our MS data also pointed out an *O*-GlcNAc site at the T306 **(Fig. 4e)** along with the previously described (35) phosphorylation showing a reciprocal phosphorylation/*O*-GlcNAcylation interplay on this residue. We also mapped two phosphorylated sites at S114 and T170 (**Supplemental Table S3 and Fig. S5**).

_O_-GlcNAcylation increases TS stability by preventing its proteasomal degradation

Since OGT and *O*-GlcNAcylation are known to control protein expression and stability (36), we investigated whether *O*-GlcNAcylation would stabilize TS. We generated series of *O*-GlcNAcylation mutants (T251A, T306A and T251A/T306A) and two phosphomimetic mutants (T306D and T251A/T306D). Level of the T251A mutant was lower than the wild type about 45% **(Fig. 5a)**. Neither the substitution of T306 to alanine (T306A) nor to aspartic acid (T306D) affected the TS expression levels compared to the wild type. The double mutant T251A/T306A exhibited a strongly decreased-level of about 75% that was restored close to wild type levels for the double mutant T251A/T306D **(Fig. 5a)**. This data suggests that *O*-GlcNAcylation at T251 and phosphorylation/*O*-GlcNAcylation interplay at T306 control TS protein level. We then performed a time-course experiment in which HT-29 cells were treated with cycloheximide with or without Thiamet-G to analyze TS stability **(Fig. 5b)**. Thiamet-G alone induces a slight decrease of TS expression and stability because of the high TS O-GlcNAcylation stoichiometry (**Fig. 4c and d**). Twenty-eight hours after cycloheximide protein synthesis inhibition, only 10% of TS remained detectable, while cells co-treatment with Thiamet-G exhibited about 20% of remaining TS **(Fig. 5b)**. This data showed that forced-enhancement of *O*-GlcNAcylation increased TS lifetime. We then analyzed TS levels after treatment with siOGT with or without the proteasome inhibitor MG132 **(Fig. 5c)**. Reduction of TS levels induced by *OGT* knockdown was partially restored upon MG132 treatment indicating that *O*-GlcNAcylation protects TS from proteasomal degradation in an ubiquitin-independent manner (37, 38) **(Fig. 5c and Supplemental Fig. S6)**. Furthermore, MG132 treatment restored protein levels of T251A and T251A-T306A mutants **(Fig. 5d)**, reinforcing the role of *O*-GlcNAcylation of these residues in the TS protection toward proteasomal degradation. Our results revealed that *O*-GlcNAcylation of TS at T251 and

O-GlcNAcylation/phosphorylation interplay at T306 regulate proteasomal degradation and stability of the enzyme. To get more insight on how PTMs affect TS stability, the full human TS protein was modeled **(Fig. 6a)** and empirical potential energies of stabilization (ΔE) of modified TS were calculated. *O*-GlcNAcylation at T306 slightly increased TS stability (ΔE = -5.8 kcal.mol^{-1}) while phosphorylation at T306 and *O*-GlcNAcylation at T251 similarly and strongly stabilized it (ΔE = -29.7 and -32.5 kcal.mol^{-1} respectively) **(Fig. 6b)**. In accordance to experimental data **(Fig. 5a)**, modification of both amino acids increased further this stability (ΔE = -42.4 and -53.2 kcal.mol^{-1} for *O*-GlcNAcylation at T251 and *O*-GlcNAcylation or phosphorylation at T306 respectively). Stabilization has originated from strong ionic and van der Waals interactions, and hydrogen bonds between TS amino acids and phosphate or *O*-GlcNAc moiety **(Fig. 6c)**. TS dimerization seems to be driven partly by *O*-GlcNAcylation since glycosylation at T251 of monomer A generates hydrogen and π-σ bonds with amino acids located in TS monomer B at the dimer interface (at G60, M61, E62, T251, L252 and Y213 residues respectively) (**Fig. 6c**). This network of links does not seem to be generated by the other structures proposed.

Discussion

5-FU alone or combined with other drugs is one of the most frequently used chemotherapy for CRC treatment. Nonetheless, the outcome is often sub-optimal because of resistance to 5-FU treatment. Since TS is a key target of 5-FU, the possible mechanism of 5-FU response in CRC is likely to involve this enzyme. Proteomic and systematic approaches identified TS as an *O*-GlcNAcylated protein (8, 9) but the role of this PTM on the enzyme remained unknown. Glycosylation alterations play an important role in CRC response to several therapies (39). To test this conjecture, we first investigated TS expression and *O*-GlcNAcylation levels in CRC tissues. Consistent with previously published data, *O*-GlcNAcylation levels are increased in colorectal tumors compared to normal tissues (40–42). AOM/DSS treatment induces tumorigenesis that activates glucose and glutamine consumption to support cell proliferation. Increased nutrient availability, subsequent flux through Hexosamine Biosynthetic Pathway (HBP) and/or OGT activity lead to hyper *O*-GlcNAcylation in tumor tissues without necessary alteration in OGT abundance (43,44). TS levels are also increased in tumors highlighting the significant need for dTMP

synthesis to support cell proliferation (45). We showed that nutrients affect TS levels by regulating *O*-GlcNAcylation and that TS *O*-GlcNAcylation is increased in colon cancer cells compared to non-cancerous ones. More interestingly, we present evidence that enhanced TS levels by *O*-GlcNAcylation sensitizes CRC to 5-FU cytotoxicity and decipher the underlying molecular mechanism. Elevation of *O*-GlcNAcylation *in vivo* by Thiamet-G correlated with increased TS levels and potentiated 5-FU cytotoxic effect in a murine model of CRC as shown by number and grade tumor analyses. We showed that Thiamet-G alone reduces CRC progression**.** It was previously shown that increased *O*-GlcNAcylation by heterozygote knockout of *Meningioma Expressed Antigen 5* (*MGEA5*) encoding OGA attenuates tumorigenesis and enhances survival in sporadic *Adenomatous Polyposis coli* (*APC*)$^{min/+}$ CRC mice model (46). Consistently with our and others' data showing that knockdown of *OGT* or *MGEA* reduces cell growth (45, 46), these studies highlight the pivotal role of *O*-GlcNAcylation homeostasis in carcinogenesis and tumor growth. Data mining of CRC patients revealed that *OGT* expression is positively correlated with the 5-FU-based chemotherapy response. Consistently, downregulation of *OGT* and *O*-GlcNAcylation decreased *in vitro* 5-FU cytotoxic effect by regulating both TS stability and levels, and subsequent cellular enzyme activity. *TYMS* gene overexpression is a currently thought to be a biomarker of 5-FU resistance in CRC (3). However, the variability of genetic background based on *TYMS* gene amplification or polymorphisms (49), transcription and translation induced by 5-FU (49–51), ratio between the FdUMP-complexed and the free form of TS (52) and final TS protein expression (53) can also modulate the sensitivity to the drug. The patient TS protein expression might result from several regulatory changes at many levels such as transcription, post-transcriptional regulation, translation, and post-translational regulation (54). Distinguishing between mRNA overexpression and enzyme post-translational stabilization as a regulation mechanism of TS proteins has implications with regard to how cancer cells may respond to 5-FU therapy. Although cells with low TS levels might theoretically be more sensitive to 5-FU, the subsequent low proliferation rate prevents induction of DNA damage and 5-FU toxicity as we show in non-cancerous CCD 841 CoN cells. In parallel, HT-29 5F31 cancer cells which exhibit high TS level due to *TYMS* gene amplification are also resistant to 5-FU. Thus, we suggest that the regulation of 5-FU response by *O*-GlcNAcylation is finely tuned and depends on a proper

amount of TS proteins. Moreover, *O*-GlcNAcylation strongly stabilizes TS by forming novel intra- and inter-monomer interactions (hydrogen and π-σ bonds). Potential PTM induced-structure modifications of TS could also increase its affinity for FdUMP metabolites and thus enhancing TS inhibition.

We also reveal a reciprocal effect of 5-FU on *O*-GlcNAcylation levels *in vitro* and *in vivo.* 5-FU treatment affected *O*-GlcNAcylation by decreasing OGT at both protein and mRNA levels in non-cancerous and 5-FU sensitive cancerous colon cell lines. In murine CRC tumors, OGT levels were steady under 5-FU treatment. This difference could be due to that OGT levels were analyzed after two weeks of systemic 5-FU treatment in mice allowing possible return to equilibrium while cell lines received 72 hours acute treatment. Additionally, the 5-FU-induced decrease of protein *O*-GlcNAcylation in murine CRC tissues could be related to decreased OGT activity rather than to decreased OGT level. Since OGT activity is inhibited by high UDP, UTP and UDP-GlcNAc concentrations (55), 5-FU metabolites may inhibit OGT by producing fluorinated derivates of uridine compounds (56). We demonstrate that 5-FU decreases *OGT* expression and cellular *O*-GlcNAcylation without affecting *O*-GlcNAcylation of TS suggesting that this PTM is abundant and/or stable. Under 5-FU treatment, the *O*-GlcNAcylation stabilizes TS whose major FdUMP-complexed isoform is inhibited leading to cell cycle arrest and apoptosis. Together, our study highlights a crosstalk between *O*-GlcNAcylation and 5-FU metabolism *in vitro* and *in vivo* which is at the benefit of stabilizing the 5-FU target TS by *O*-GlcNAcylation, hence enhancing the sensitivity to 5-FU.

We show here that TS *O*-GlcNAcylation at T251 and T306 stabilizes the enzyme by preventing its proteasomal degradation in ubiquitin-independent pathway. TS proteasomal degradation is controlled by two degron sequences M1-R42 and F276-V313 located respectively in the N- (N-ter) and C-terminal (C-ter) regions (57). We report for the first time an *O*-GlcNAc modification at T251, a key residue located in the sixth β-strand at the dimer interface of TS (58). We show that the T251A mutation decreases TS stability. Recently, Pozzi et al. (2019) showed that the substitution of Q62N at the dimer interface destabilizes TS homodimer by inducing a slight aperture of the TS dimer (59). In a similar manner, the T251A mutation could decrease stability of TS by modifying *O*-GlcNAc induced-interactions and reducing its dimerization. Interestingly, T306 is located within

373 the C-ter cryptic degron whose activity is regulated by the N-ter degron (57). The sole mutation T306A does not
374 affect TS stability in accordance with the observation that deletion of P305-I307 sequence comprising the T306
375 residue does not affect stability of TS (38). Conversely, in combination with T251A mutation the absence of
376 modification at T306 enhances TS degradation. This result is reinforced by our data showing that the T306D
377 phosphomimetic mutation is able to restore stability of T251A mutants suggesting that phosphorylation of this
378 site would inhibit the TS degron activity. Remarkably, the P305-I307 sequence of TS is similar to the
379 P375-T-L377 tripeptide motif that dictates the ubiquitin-independent degradation of c-Fos protein.
380 Degradation of c-Fos depends on the activity of N-ter and C-ter degrons that are regulated by phosphorylation
381 and possibly by heterodimerization of c-Fos with various partners, the best known being the Jun family
382 members (60). TS degron activity could also be regulated by PTMs and dimerization. Here, we report that the
383 T251A mutation decreases TS stability that can be restored by phosphorylation at T306, indicating that TS
384 proteasomal degradation driven by hypo-*O*-GlcNAcylation at T251 depends on
385 *O*-GlcNAcylation/phosphorylation status at T306 of the C-ter degron. Relative empirical potential stabilization
386 energy calculations indicate that both *O*-GlcNAcylation and phosphorylation at T306 increases stability of T251
387 *O*-GlcNAcylated TS.
388 In agreement with our findings, the beneficial effect of *O*-GlcNAcylation in response to chemotherapy has also
389 been documented for cisplatin in ovarian cancer (16,17), for bortezomib in mantle cell lymphoma (19) and for
390 TRAIL therapy in various cancers (14). Thiamet-G is the most widely used OGA inhibitor *in vitro* and *in vivo* as it
391 exhibits excellent stability and selectivity (61). Two others selective OGA inhibitors (MK-8719 and ASN120290)
392 have been recently included in the orphan drug designation program of the US Food and Drug Administration
393 for the safe and effective treatment of the progressive supranuclear palsy, a neurodegenerative tauopathy. Our
394 study shows that *O*-GlcNAc homeostasis-TS axis plays an important role in mediating 5-FU sensitivity in CRC,
395 hence therapeutic combination strategy of 5-FU with an OGA inhibitor would be beneficial for CRC patients.
396 More broadly, several existing potent inhibitors of HBP enzymes, OGT and OGA have shown interests in

anti-cancer therapies (62). Therefore, targeting *O*-GlcNAcylation in combination with chemotherapy in pre-clinical models should be explored further.

For summarize, in this paper, we show that a combined treatment of 5-FU with Thiamet-G has a synergistic inhibitory effect on CRC progression. We evidence a crosstalk between *O*-GlcNAcylation, TS and 5-FU cytotoxicity. We report that *O*-GlcNAcylation stabilizes the human TS and sensitizes to 5-FU effect. We in-depth document the *O*-GlcNAc T251 site-specific function along with its interplay with phospho/*O*-GlcNAc T306 on TS structure and stability. Since, resistance to 5-FU is the major obstacle to therapy success, comprehension of molecular mechanism of TS regulation that potentiates 5-FU effectiveness is of high importance to open a new paradigm of cancer therapeutic options.

Acknowledgments

This work was supported by the “Ligue Contre le Cancer/Comité du Nord/Comité de la Somme”, the “Région Hauts-de-France” (Cancer Regional Program), the University of Lille and the “Centre National de la Recherche Scientifique”. NV is the recipient of a fellowship from the “Ministère de l’Enseignement Supérieur et de la Recherche”. The authors acknowledge the financial support from ITMO Cancer AVIESAN (Alliance Nationale pour les Sciences de la Vie et de la Santé, National Alliance for Life Sciences and Health) within the framework of the cancer plan for Orbitrap mass spectrometer funding.

We thank Dr. Guillemette Huet (CANTHER UMR9020 UMR1277, Lille, France) for HT-29 5F31 cell line (23), Dr. Matthew G. Alteen (Department of Chemistry, Simon Fraser University, Canada) for Thiamet-G and Dr. Cyril Couturier (UMR8090 IBL, Lille, France) for pcDNA3.1-Ub-HA plasmid gifts.

Author contributions

NV designed, performed and analyzed *in vitro* and *in vivo* experiment data and co-wrote the manuscript. SH performed plasmid constructions and PEG synthesis and cowrote the manuscript. AD contributed to the *in vivo* experiments. JKC contributed to the *in vivo* experiment design and the reviewing of the manuscript. JT

contributed to the *in vivo* experiments. MD performed mice colonoscopy and contributed to the IHC experiments. AP performed mass spectrometry analyzes. GV performed TS structure modeling in silico analysis. CS performed microscopy acquisition of fluorescence images of immunocytochemistry experiments. TL contributed to discussions and reviewed the manuscript. VD contributed to the work design, the experiments, the data analysis and the reviewing of the manuscript. IEB supervised and conceptualized the research, contributed to the experiments and data analyzes, and co-wrote the manuscript. All authors read and approved the manuscript.

Correspondence and requests for materials should be addressed to Ikram El Yazidi-Belkoura, Université de Lille, CNRS, UMR8576 - UGSF - Unité de Glycobiologie Structurale et Fonctionnelle, F-59000, Lille, France.

ikram.el-yazidi@univ-lille.fr

Competing Interests

No potential conflicts of interest were disclosed.

References

1. Ishikawa M, Miyauchi T, Kashiwagi Y. Clinical implications of thymidylate synthetase, dihydropyrimidine dehydrogenase and orotate phosphoribosyl transferase activity levels in colorectal carcinoma following radical resection and administration of adjuvant 5-FU chemotherapy. BMC Cancer. 2 juill 2008;8(1):188.

2. Kristensen MH, Weidinger M, Bzorek M, Pedersen PL, Mejer J. Correlation between thymidylate synthase gene variants, RNA and protein levels in primary colorectal adenocarcinomas. J Int Med Res. avr 2010;38(2):484‑97.

3. Palmirotta R, Carella C, Silvestris E, Cives M, Stucci SL, Tucci M, et al. SNPs in predicting clinical efficacy and toxicity of chemotherapy: walking through the quicksand. Oncotarget. 16 avr 2018;9(38):25355‑82.

4. Wakasa K, Kawabata R, Nakao S, Hattori H, Taguchi K, Uchida J, et al. Dynamic Modulation of Thymidylate Synthase Gene Expression and Fluorouracil Sensitivity in Human Colorectal Cancer Cells. PLoS One. 16 avr 2015;10(4):e0123076.

5. Samsonoff WA, Reston J, McKee M, O'Connor B, Galivan J, Maley G, et al. Intracellular location of thymidylate synthase and its state of phosphorylation. J Biol Chem. 16 mai 1997;272(20):13281‑5.

6. Fraczyk T, Kubiński K, Masłyk M, Cieśla J, Hellman U, Shugar D, et al. Phosphorylation of thymidylate synthase from various sources by human protein kinase CK2 and its catalytic subunits. Bioorg Chem. juin 2010;38(3):124‑31.

7. Anderson DD, Woeller CF, Stover PJ. Small ubiquitin-like modifier-1 (SUMO-1) modification of thymidylate synthase and dihydrofolate reductase. Clin Chem Lab Med. 2007;45(12):1760‑3.

8. Peña MMO, Melo SP, Xing Y-Y, White K, Barbour KW, Berger FG. The Intrinsically Disordered N-terminal Domain of Thymidylate Synthase Targets the Enzyme to the Ubiquitin-independent Proteasomal Degradation Pathway. J Biol Chem. 13 nov 2009;284(46):31597‑607.

9. Hahne H, Sobotzki N, Nyberg T, Helm D, Borodkin VS, van Aalten DM, et al. Proteome wide purification and identification of O-GlcNAc modified proteins using Click chemistry and mass spectrometry. J Proteome Res. 1 févr 2013;12(2):927‑36.

10. Sprung R, Nandi A, Chen Y, Kim SC, Barma D, Falck JR, et al. Tagging-via-Substrate Strategy for Probing O-GlcNAc Modified Proteins. J Proteome Res. juin 2005;4(3):950‑7.

11. Yang X, Qian K. Protein O -GlcNAcylation: emerging mechanisms and functions. Nature Reviews Molecular Cell Biology. juill 2017;18(7):452‑65.

12. Hanover JA, Chen W, Bond MR. O-GlcNAc in cancer: An Oncometabolism-fueled vicious cycle. J Bioenerg Biomembr. 2018;50(3):155‑73.

13. Kanwal S, Fardini Y, Pagesy P, N'tumba-Byn T, Pierre-Eugène C, Masson E, et al. O-GlcNAcylation-inducing treatments inhibit estrogen receptor α expression and confer resistance to 4-OH-tamoxifen in human breast cancer-derived MCF-7 cells. PLoS ONE. 2013;8(7):e69150.

14. Lee H, Oh Y, Jeon Y-J, Lee S-Y, Kim H, Lee H-J, et al. DR4-Ser424 O-GlcNAcylation Promotes Sensitization of TRAIL-Tolerant Persisters and TRAIL-Resistant Cancer Cells to Death. Cancer Res. 1 juin 2019;79(11):2839‑52.

15. Yang S-Z, Xu F, Yuan K, Sun Y, Zhou T, Zhao X, et al. Regulation of pancreatic cancer TRAIL resistance by protein O-GlcNAcylation. Lab Invest. 2 janv 2020;

16. Zhou F, Yang X, Zhao H, Liu Y, Feng Y, An R, et al. Down-regulation of OGT promotes cisplatin resistance by inducing autophagy in ovarian cancer. Theranostics. 6 oct 2018;8(19):5200‑12.

17. de Queiroz RM, Madan R, Chien J, Dias WB, Slawson C. Changes in O-Linked N-Acetylglucosamine (O-GlcNAc) Homeostasis Activate the p53 Pathway in Ovarian Cancer Cells. J Biol Chem. 2 sept 2016;291(36):18897‑914.

18. Luanpitpong S, Angsutararux P, Samart P, Chanthra N, Chanvorachote P, Issaragrisil S. Hyper- O -GlcNAcylation induces cisplatin resistance via regulation of p53 and c-Myc in human lung carcinoma. Scientific Reports. 6 sept 2017;7(1):10607.

19. Luanpitpong S, Chanthra N, Janan M, Poohadsuan J, Samart P, U-Pratya Y, et al. Inhibition of O-GlcNAcase sensitizes apoptosis and reverses bortezomib resistance in mantle cell lymphoma through modification of truncated Bid. Mol Cancer Ther. févr 2018;17(2):484‑96.

20. Sekine H, Okazaki K, Kato K, Alam MM, Shima H, Katsuoka F, et al. O-GlcNAcylation Signal Mediates Proteasome Inhibitor Resistance in Cancer Cells by Stabilizing NRF1. Mol Cell Biol. 01 2018;38(17).

21. Xie X, Wu Q, Zhang K, Liu Y, Zhang N, Chen Q, et al. O-GlcNAc regulates MTA1 transcriptional activity during breast cancer cells genotoxic adaptation. bioRxiv. 8 févr 2021;2021.02.08.430201.

22. Kang KA, Piao MJ, Ryu YS, Kang HK, Chang WY, Keum YS, et al. Interaction of DNA demethylase and histone methyltransferase upregulates Nrf2 in 5-fluorouracil-resistant colon cancer cells. Oncotarget. 31 mai 2016;7(26):40594‑620.

23. Lesuffleur T, Kornowski A, Luccioni C, Muleris M, Barbat A, Beaumatin J, et al. Adaptation to 5-fluorouracil of the heterogeneous human colon tumor cell line HT-29 results in the selection of cells committed to differentiation. Int J Cancer. 11 nov 1991;49(5):721‑30.

24. Becker C, Fantini MC, Wirtz S, Nikolaev A, Kiesslich R, Lehr HA, et al. In vivo imaging of colitis and colon cancer development in mice using high resolution chromoendoscopy. Gut. juill 2005;54(7):950‑4.

25. Hardivillé S, Banerjee PS, Selen Alpergin ES, Smith DM, Han G, Ma J, et al. TATA-Box Binding Protein O-GlcNAcylation at T114 Regulates Formation of the B-TFIID Complex and Is Critical for Metabolic Gene Regulation. Molecular Cell. 5 mars 2020;77(5):1143-1152.e7.

26. Etienne M-C, Ilc K, Formento J-L, Laurent-Puig P, Formento P, Cheradame S, et al. Thymidylate synthase and methylenetetrahydrofolate reductase gene polymorphisms: relationships with 5-fluorouracil sensitivity. Br J Cancer. 26 janv 2004;90(2):526‑34.

27. Decourcelle A, Very N, Djouina M, Loison I, Thévenet J, Body-Malapel M, et al. O-GlcNAcylation Links Nutrition to the Epigenetic Downregulation of UNC5A during Colon Carcinogenesis. Cancers (Basel) [Internet]. 28 oct 2020 [cité 5 avr 2021];12(11). Disponible sur: https://www.ncbi.nlm.nih.gov/pmc/articles/PMC7693889/

28. Almog R, Waddling CA, Maley F, Maley GF, Van Roey P. Crystal structure of a deletion mutant of human thymidylate synthase Δ (7–29) and its ternary complex with Tomudex and dUMP. Protein Sci. mai 2001;10(5):988‑96.

29. Jorgensen WL, Tirado-Rives J. Molecular modeling of organic and biomolecular systems using BOSS and MCPRO. J Comput Chem. déc 2005;26(16):1689‑700.

30. Vergoten G, Mazur I, Lagant P, Michalski JC, Zanetta JP. The SPASIBA force field as an essential tool for studying the structure and dynamics of saccharides. Biochimie. 1 janv 2003;85(1):65‑73.

31. Lagant P, Nolde D, Stote R, Vergoten G, Karplus M. Increasing Normal Modes Analysis Accuracy: The SPASIBA Spectroscopic Force Field Introduced into the CHARMM Program. J Phys Chem A. 1 mai 2004;108(18):4019‑29.

32. Stastna M, Janeckova L, Hrckulak D, Kriz V, Korinek V. Human Colorectal Cancer from the Perspective of Mouse Models. Genes (Basel) [Internet]. 11 oct 2019 [cité 5 mai 2020];10(10). Disponible sur: https://www.ncbi.nlm.nih.gov/pmc/articles/PMC6826908/

33. Decourcelle A, Loison I, Baldini S, Leprince D, Dehennaut V. Evidence of a compensatory regulation of colonic O-GlcNAc transferase and O-GlcNAcase expression in response to disruption of O-GlcNAc homeostasis. Biochemical and Biophysical Research Communications. 1 janv 2020;521(1):125‑30.

34. Peters GJ, van der Wilt CL, van Triest B, Codacci-Pisanelli G, Johnston PG, van Groeningen CJ, et al. Thymidylate synthase and drug resistance. Eur J Cancer. août 1995;31A(7‑8):1299‑305.

35. Frączyk T, Ruman T, Wilk P, Palmowski P, Rogowska-Wrzesinska A, Cieśla J, et al. Properties of phosphorylated thymidylate synthase. Biochimica et Biophysica Acta (BBA) - Proteins and Proteomics. déc 2015;1854(12):1922‑34.

36. Ruan H-B, Nie Y, Yang X. Regulation of Protein Degradation by O-GlcNAcylation: Crosstalk with Ubiquitination. Mol Cell Proteomics. déc 2013;12(12):3489‑97.

37. Forsthoefel AM, Peña MMO, Xing YY, Rafique Z, Berger FG. Structural determinants for the intracellular degradation of human thymidylate synthase. Biochemistry. 24 févr 2004;43(7):1972‑9.

38. Peña MMO, Xing YY, Koli S, Berger FG. Role of N-terminal residues in the ubiquitin-independent degradation of human thymidylate synthase. Biochem J. 15 févr 2006;394(Pt 1):355‑63.

39. Very N, Lefebvre T, El Yazidi-Belkoura I. Drug resistance related to aberrant glycosylation in colorectal cancer. Oncotarget. 3 nov 2017;9(1):1380‑402.

40. Mi W, Gu Y, Han C, Liu H, Fan Q, Zhang X, et al. O-GlcNAcylation is a novel regulator of lung and colon cancer malignancy. Biochim Biophys Acta. avr 2011;1812(4):514‑9.

41. Olivier-Van Stichelen S, Dehennaut V, Buzy A, Zachayus J-L, Guinez C, Mir A-M, et al. O-GlcNAcylation stabilizes β-catenin through direct competition with phosphorylation at threonine 41. FASEB J. août 2014;28(8):3325‑38.

42. Yu M, Chu S, Fei B, Fang X, Liu Z. O-GlcNAcylation of ITGA5 facilitates the occurrence and development of colorectal cancer. Exp Cell Res. 15 sept 2019;382(2):111464.

43. Singh JP, Qian K, Lee J-S, Zhou J, Han X, Zhang B, et al. O-GlcNAcase targets pyruvate kinase M2 to regulate tumor growth. Oncogene. janv 2020;39(3):560‑73.

44. Raab S, Gadault A, Very N, Decourcelle A, Baldini S, Schulz C, et al. Dual regulation of fatty acid synthase (FASN) expression by O-GlcNAc transferase (OGT) and mTOR pathway in proliferating liver cancer cells. Cell Mol Life Sci. juill 2021;78(13):5397‑413.

45. Rahman L, Voeller D, Rhaman M, Lipkowitz S, Allegra C, Barrett J, et al. Thymidylate synthase as an oncogene: a novel role for an essential DNA synthesis enzyme. - PubMed - NCBI. Cancer Cell. avr 2004;5(4):341‑51.

46. Yang YR, Jang H-J, Yoon S, Lee YH, Nam D, Kim IS, et al. OGA heterozygosity suppresses intestinal tumorigenesis in Apcmin/+ mice. Oncogenesis. juill 2014;3(7):e109.

47. Steenackers A, Olivier-Van Stichelen S, Baldini SF, Dehennaut V, Toillon R-A, Le Bourhis X, et al. Silencing the Nucleocytoplasmic O-GlcNAc Transferase Reduces Proliferation, Adhesion, and Migration of Cancer and Fetal Human Colon Cell Lines. Front Endocrinol (Lausanne) [Internet]. 25 mai 2016 [cité 5 janv 2020];7. Disponible sur: https://www.ncbi.nlm.nih.gov/pmc/articles/PMC4879930/

48. Yang YR, Song M, Lee H, Jeon Y, Choi E-J, Jang H-J, et al. O-GlcNAcase is essential for embryonic development and maintenance of genomic stability. Aging Cell. 2012;11(3):439‑48.

49. Xi Y, Nakajima G, Schmitz JC, Chu E, Ju J. Multi-level gene expression profiles affected by thymidylate synthase and 5-fluorouracil in colon cancer. BMC Genomics. 3 avr 2006;7:68.

50. Peters GJ, Backus HHJ, Freemantle S, van Triest B, Codacci-Pisanelli G, van der Wilt CL, et al. Induction of thymidylate synthase as a 5-fluorouracil resistance mechanism. Biochim Biophys Acta. 18 juill 2002;1587(2‑3):194‑205.

51. Nishiyama M, Yamamoto W, Park JS, Okamoto R, Hanaoka H, Takano H, et al. Low-dose cisplatin and 5-fluorouracil in combination can repress increased gene expression of cellular resistance determinants to themselves. Clin Cancer Res. sept 1999;5(9):2620‑8.

52. Swain SM, Lippman ME, Egan EF, Drake JC, Steinberg SM, Allegra CJ. Fluorouracil and high-dose leucovorin in previously treated patients with metastatic breast cancer. JCO. 1 juill 1989;7(7):890‑9.

53. Gajjar. Influence of thymidylate synthase expression on survival in patients with colorectal cancer [Internet]. [cité 25 août 2021]. Disponible sur: https://www.ijamhrjournal.org/article.asp?issn=2349-4220;year=2017;volume=4;issue=2;spage=61;epage=68;aulast=Gajjar

54. Bai W, Wu Y, Zhang P, Xi Y. Correlations between expression levels of thymidylate synthase, thymidine phosphorylase and dihydropyrimidine dehydrogenase, and efficacy of 5-fluorouracil-based chemotherapy for advanced colorectal cancer. Int J Clin Exp Pathol. 1 oct 2015;8(10):12333‑45.

55. Haltiwanger RS, Blomberg MA, Hart GW. Glycosylation of nuclear and cytoplasmic proteins. Purification and characterization of a uridine diphospho-N-acetylglucosamine:polypeptide beta-N-acetylglucosaminyltransferase. J Biol Chem. 5 mai 1992;267(13):9005‑13.

56. Pederson NV, Zanghi JA, Miller WM, Knop RH. Discrimination of fluorinated uridine metabolites in N-417 small cell lung cancer cell extracts via 19F- and 31P-NMR. Magn Reson Med. févr 1994;31(2):224‑8.

57. Barbour KW, Xing Y-Y, Peña EA, Berger FG. Characterization of the bipartite degron that regulates ubiquitin-independent degradation of thymidylate synthase. Biosci Rep [Internet]. 18 janv 2013;33(1). Disponible sur: https://www.ncbi.nlm.nih.gov/pmc/articles/PMC3549573/

58. Chanama S, Chitnumsub P, Leartsakulpanich2 U, Chanama M. Distinct dimer interface of Plasmodium falciparum thymidylate synthase: Implication for species-specific antimalarial drug design. The Southeast Asian journal of tropical medicine and public health. juill 2017;48(4):722‑36.

59. Pozzi C, Lopresti L, Santucci M, Costi MP, Mangani S. Evidence of Destabilization of the Human Thymidylate Synthase (hTS) Dimeric Structure Induced by the Interface Mutation Q62R. Biomolecules [Internet]. 3 avr 2019 [cité 19 août 2020];9(4). Disponible sur: https://www.ncbi.nlm.nih.gov/pmc/articles/PMC6523895/

60. Ferrara P, Andermarcher E, Bossis G, Acquaviva C, Brockly F, Jariel-Encontre I, et al. The structural determinants responsible for c-Fos protein proteasomal degradation differ according to the conditions of expression. Oncogene. mars 2003;22(10):1461‑74.

61. Yuzwa SA, Macauley MS, Heinonen JE, Shan X, Dennis RJ, He Y, et al. A potent mechanism-inspired O-GlcNAcase inhibitor that blocks phosphorylation of tau in vivo. Nat Chem Biol. août 2008;4(8):483‑90.

62. Lam C, Low J-Y, Tran PT, Wang H. The hexosamine biosynthetic pathway and cancer: Current knowledge and future therapeutic strategies. Cancer Lett. 20 janv 2021;503:11‑8.

Figure legends

Fig. 1. *O*-GlcNAcylation sensitizes CRC to 5-FU chemotherapy *in vivo*. a-f Colorectal tumors were induced by AOM/DSS and continuously treated with Thiamet-G (90 mg/kg/d) and/or 5-FU (12,5 mg/kg/d) during 13 days. Colonoscopy was performed before sacrifice. **a** Representative endoscopic images of tumors. **b** Quantification of tumor number as observed by endoscopy. Data is median ± SEM, n≥6. **c** Quantification of tumor number by grade as observed and scored by endoscopy. Data is mean ± SEM, n≥6. **d** Histogram quantification of percentage of mice with the tumor indicated highest grade. **e** Levels of OGT, *O*-GlcNAcylation and TS in tumors. Samples were immunoblotted with indicated antibodies (*left panel*). Densitometric analysis (*right panel*). Data is mean ± SEM, n≥6. **f** Immunohistochemistry of *O*-GlcNAcylation and TS in tumors. Samples were stained with indicated antibodies. Scale bars = 50 µm (*left panel*). Staining intensity analysis in epithelial cells and scoring (*right panel*). Data is mean ± SEM, n≥3. **a-f** * $P < 0.05$, ** $P < 0.01$, *** $P < 0.001$, one-way ANOVA test. **g** Expression levels of *OGT* and *TYMS* in responder and non-responder metastatic CRC patients treated with first line 5-FU-based chemotherapy from microarray dataset GSE104645. Data was normalized by the percentile shift (all samples were normalized to the signal value of 75th percentile of all of probes on the microarray) and the scaling (all genes were normalized to the median of all samples). Data is median ± SEM**;** ** $P < 0.01$; Mann-Whitney test.

Fig. 2. 5-FU decreases OGT and *O*-GlcNAcylation levels in non-cancerous and cancerous cells. a OGT, *O*-GlcNAcylation and TS protein levels in CCD 841 CoN, HT-29, and HT-29 5F31 cells. Samples were immunoblotted with indicated antibodies (*left panel*). Densitometric analysis (*right panel*). Data is mean ± SD, n=3. **b** 5-FU IC_{50} values for CCD 841 CoN, HT-29 and HT-29 5F31 cells as determined by the MTS assay. Cells were treated 48 h by increasing concentrations of 5-FU ranging from 0 to 20 µM for CCD 841 CoN and HT-29 cells, and from 0 to 50 mM for HT-29 5F31 cells. Data is mean ± SD, n=3. **c** Effect of 5-FU on OGT, *O*-GlcNAcylation and TS protein levels. Cells were treated with or without 5-FU (6 µM) for 0, 24 h, 48 h or 72 h. Samples were immunoblotted with indicated antibodies (*top panel*). Densitometric analysis (*bottom panel*).

628 Data is mean ± SD, n=3. **a and c** * $P < 0.05$, ** $P < 0.01$, *** $P < 0.001$, one-way ANOVA test. **d** Effect of 5-FU on
629 OGT expression. Gene expression levels of OGT were determined by RT-qPCR in cells treated with or without 5-
630 FU (6 µM) for 72 h. Data is expressed as relative expression. ** $P < 0.01$, *** $P < 0.001$, unpaired Student's *t*
631 test.
632
633 **Fig. 3. Knockdown of *OGT* reduces 5-FU sensitivity of cancer cells by decreasing TS target levels. a, b and d**
634 Cells were transfected with control or *OGT* siRNA (siCtrl or siOGT; 10 nM). Then, 24 hours later, cells were
635 co-treated with or without 5-FU (6 µM) for 72 h. **a** Effects of siOGT and 5-FU treatments on OGT,
636 *O*-GlcNAcylation, PARP-1 and TS levels were evaluated by WB (*left panel*). Densitometric analysis (*right panels*).
637 Data is mean ± SD, n=3. **b** Effect of siOGT and 5-FU treatments on cellular TS activity was analyzed by
638 radioactive tritium-release assay. Data is mean ± SD, n=3. **c** Effect of siOGT and 5-FU treatment on TS
639 transcriptional levels. Gene expression level of *TYMS* was determined by RT-qPCR and data are represented as
640 relative expression. Data is mean ± SD, n=3. **d** Effect of siOGT on 5-FU IC_{50} was analyzed by MTS assay. Cells
641 were transfected with control or *OGT* siRNA (siCtrl or siOGT; 10 nM) for 24 h and then co-treated or not for 72
642 h with increasing concentrations of 5-FU ranging from 0 to 80 µM for CCD 841 CoN and HT-29 cells and from 0
643 to 50 mM for HT-29 5F31 cells. Dose response curve to 5-FU treatment (*left panel*) and 5-FU IC_{50} value
644 comparisons (*right panel*)
645 Data is mean ± SD, n=3. ** $P < 0.01$, unpaired Student's *t* test. **e-f** Effect of TS overexpression on
646 siOGT-regulated apoptosis in 5-FU sensitive HT-29 cells. HT-29 cells were first transfected with indicated siRNA.
647 After 24 h, cells were transfected with the indicated constructs and treated with 5-FU (6 µM) for 72 h prior to
648 lysis. **e** OGT, *O*-GlcNAcylation, TS-3xFLAG and TS WB. **f** $SubG_1$ apoptotic cell population was analyzed by FACS
649 after propidium iodide incorporation. Data is mean ± SD, n=4. **a, b, d and f** * $P < 0.05$, ** $P < 0.01$, *** $P <$
650 0.001, one-way ANOVA test.
651

Fig. 4. OGT interacts with and *O*-GlcNAcylates TS. a *O*-GlcNAcylation regulates TS protein levels. Prior to conducting the experiment, HT-29 cells were grown in low glucose (LG, 5 mM) medium for 60 h, then in medium without glucose (0G) supplemented with or without glucosamine ($GlcNH_2$, 5 mM) or LG or high glucose (HG, 25 mM) medium for 12 h. In transfection experiment cells were transfected in LG medium with control or *OGT* siRNA (siCtrl or siOGT; 10 nM) and, 24 h later, grown in HG medium during the last 48 hours. Samples were immunoblotted with indicated antibodies (*left panel*). Densitometric analysis (*right panel*). Data is mean ± SD, n=3**;** * $P < 0.05$, *** $P < 0.001$, one-way ANOVA test. **b-d** Cells were treated with or without 5-FU (6 µM) for 48 h. **b** OGT interacts with TS. TS and OGT were co-immunoprecipitated from HT-29 5F31 lysates and samples were immunoblotted with indicated antibodies. **c** OGT *O*-GlcNAcylates TS. HT-29 cells were transfected with siCtrl or siOGT (10 nM) and, 24 h later, incubated with or without 5-FU (6 µM) for 72 h. TS was immunoprecipitated from HT-29 cell lysates and samples were immunoblotted with indicated antibodies. **d** *O*-GlcNAc stoichiometry of TS. CCD 841 CoN and HT-29 cell lysates were *O*-GlcNAc mass tagged by click-chemistry using a PEG tag of 4,4 kDa. Samples were immunoblotted for TS (*top left panel*). Densitometric curves are shown in *bottom left panel* and densitometric analyses are presented in *top right panel*. Data is mean ± SD, n=2. * $P < 0.05$, one-way ANOVA test. **e** TS is *O*-GlcNAcylated at T251 and T306. HT-29 and HT-29 5F31 cells were treated with Thiamet-G (2 µM) for 48 h. HCD-MS/MS spectrum of peptides covering the T251 and T306 *O*-GlcNAcylated sites of TS. The modification sites on TS are indicated in red in the peptide sequence.

Fig. 5. *O*-GlcNAcylation at T251 and T306 increases TS stability by preventing its proteasomal degradation. a Expression levels of *O*-GlcNAc-TS mutants. HT-29 cells were transfected with empty pcDNA3.1 (mock), pcDNA3.1-3xFLAG-TYMS or the indicated mutant (1 µg) for 48 h. TS-FLAG proteins were detected by WB with the anti-FLAG antibody (*top panel*). Densitometric analysis (*bottom panel*). Data is mean ± SD, n=4. **b** *O*-GlcNAcylation increases TS stability. HT-29 cells were treated or not with Thiamet-G (2 µM) and/or cycloheximide (90 µg/mL) for 0, 20 h, 24 h, 28 h or 32 h. Samples were immunoblotted with indicated antibodies (*left panel*). Densitometric analysis (*right panel*). Data is mean ± SD, n=3. **c** *OGT* knockdown induced-

TS decrease is dependent on proteasomal degradation. HT-29 cells were transfected with control or *OGT* siRNA (siCtrl or siOGT, 10 µM) and then, 84 h later, treated or not with MG132 (10 µM) for 12 h prior lysis. Samples were immunoblotted with indicated antibodies (*left panel*). Densitometric analysis (*right panel*). Data is mean ± SD, n=3. **d** Expression level of TS-*O*-GlcNAc mutants under proteasome inhibition. HT-29 cells were transfected with the indicated construct and then, treated or not after 36 h with MG132 for 12 h prior lysis. Samples were immunoblotted with indicated antibodies (*left panel*). Densitometric analysis (*right panel*). Data is mean ± SD, n=3. **a and d** * $P < 0.05$, ** $P < 0.01$, *** $P < 0.001$, one-way ANOVA test. **b-c** * $P < 0.05$, unpaired Student's *t* test.

Fig. 6. *O*-GlcNAcylation at T251 and T306 increases TS dimer stabilization by generating intra- and inter-monomer interactions. a 3D modeling of human TS dimer structure. TS dimer crystal structure (green, PDB: IHZW) was completed with reconstituted M1-G29 (purple) and I307-V313 (red) sequences. **b** Empirical potential energies of stabilization of TS dimer whose monomer A is modified at T251 and T306 residues relative to unmodified TS dimer. **c** 2D view of interactions of GlcNAc or phosphate moiety at T251 and T306 residues of the monomer A with surrounding amino acids of monomers A and B.

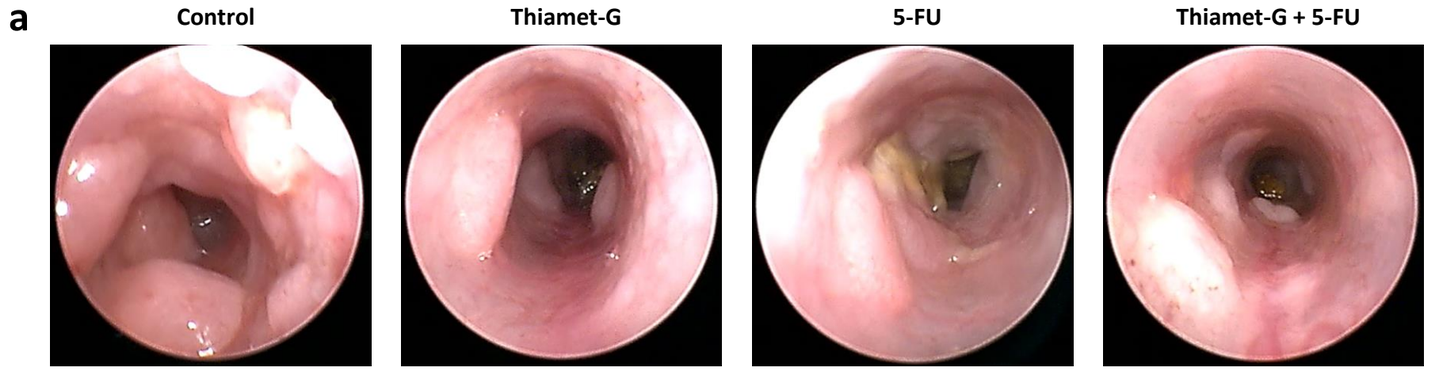

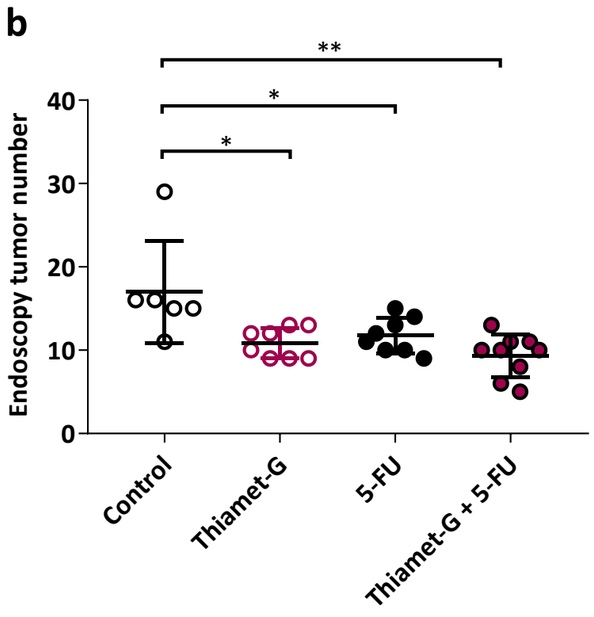

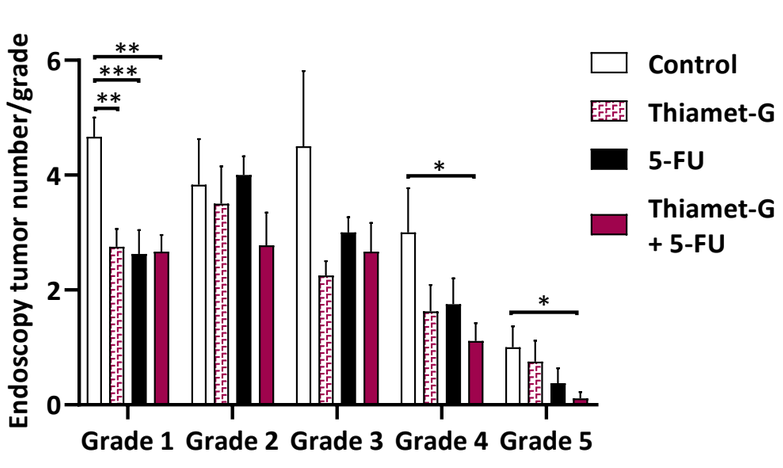

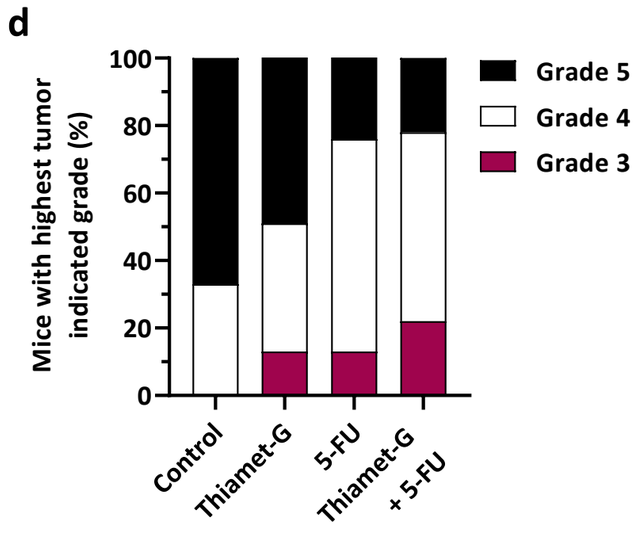

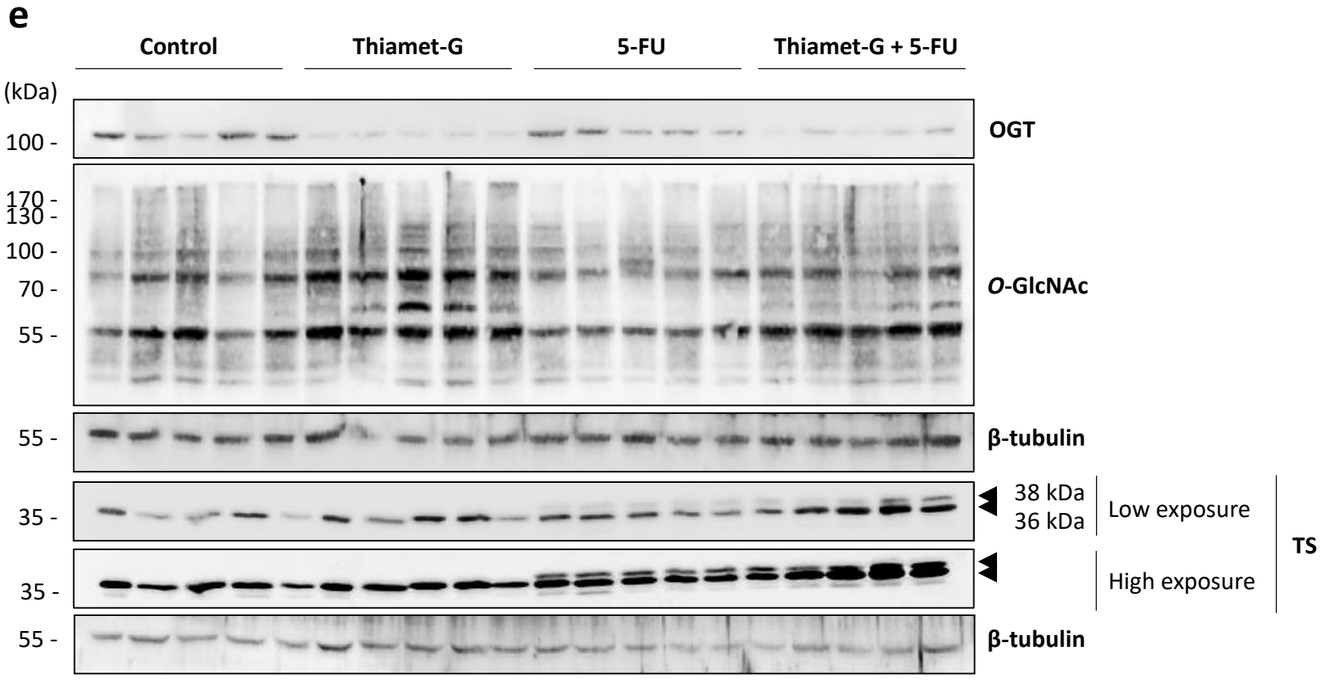

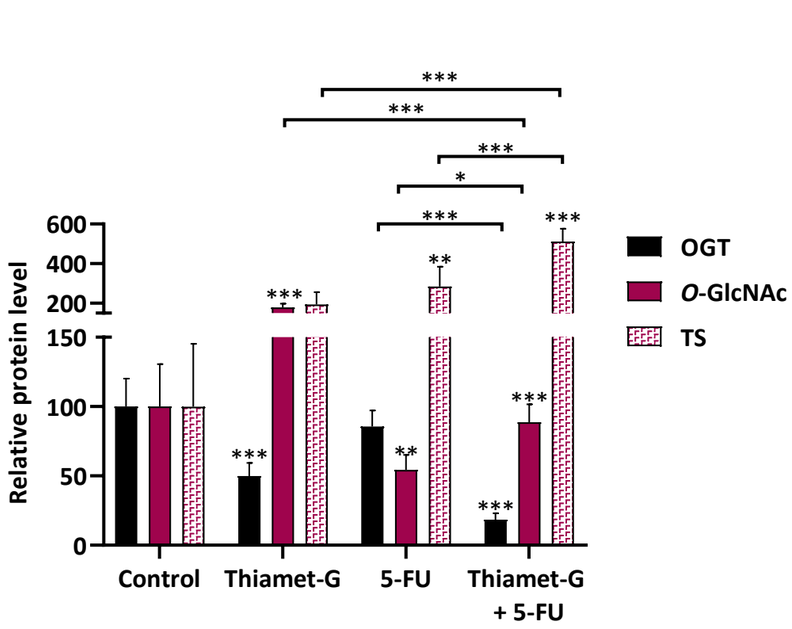

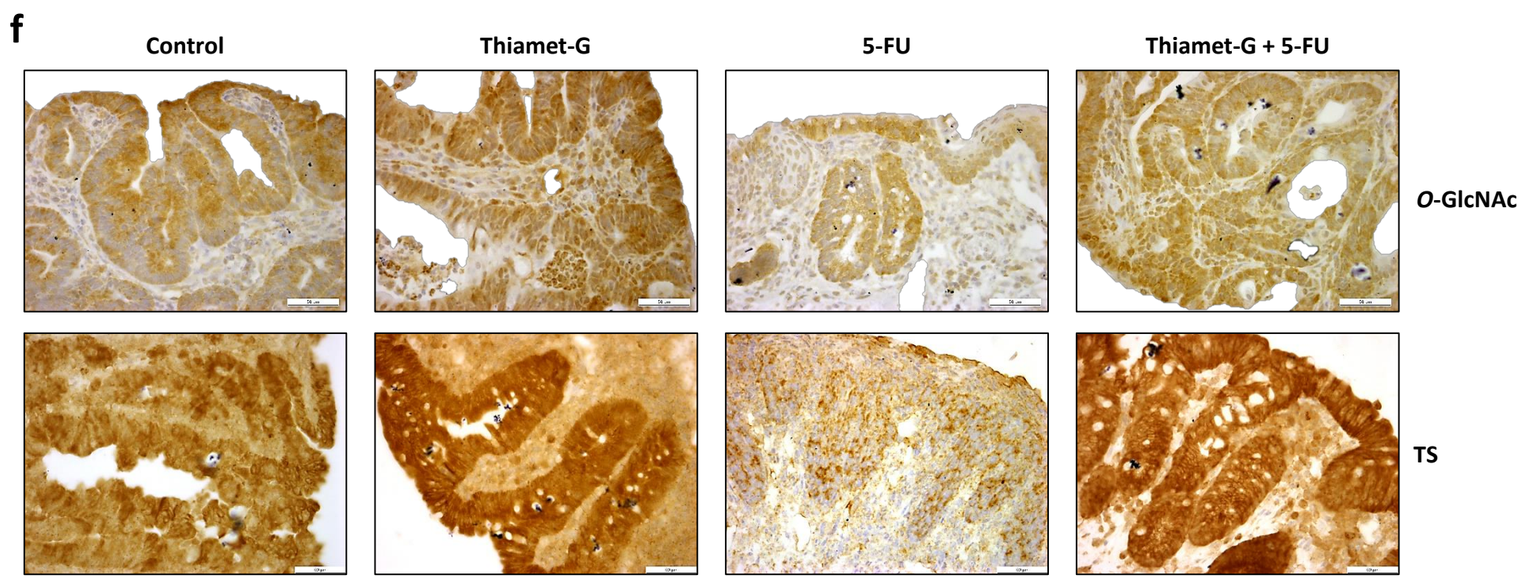

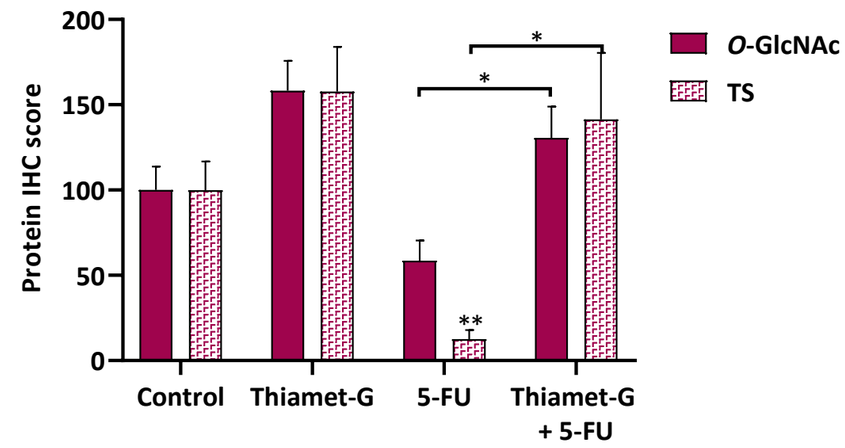

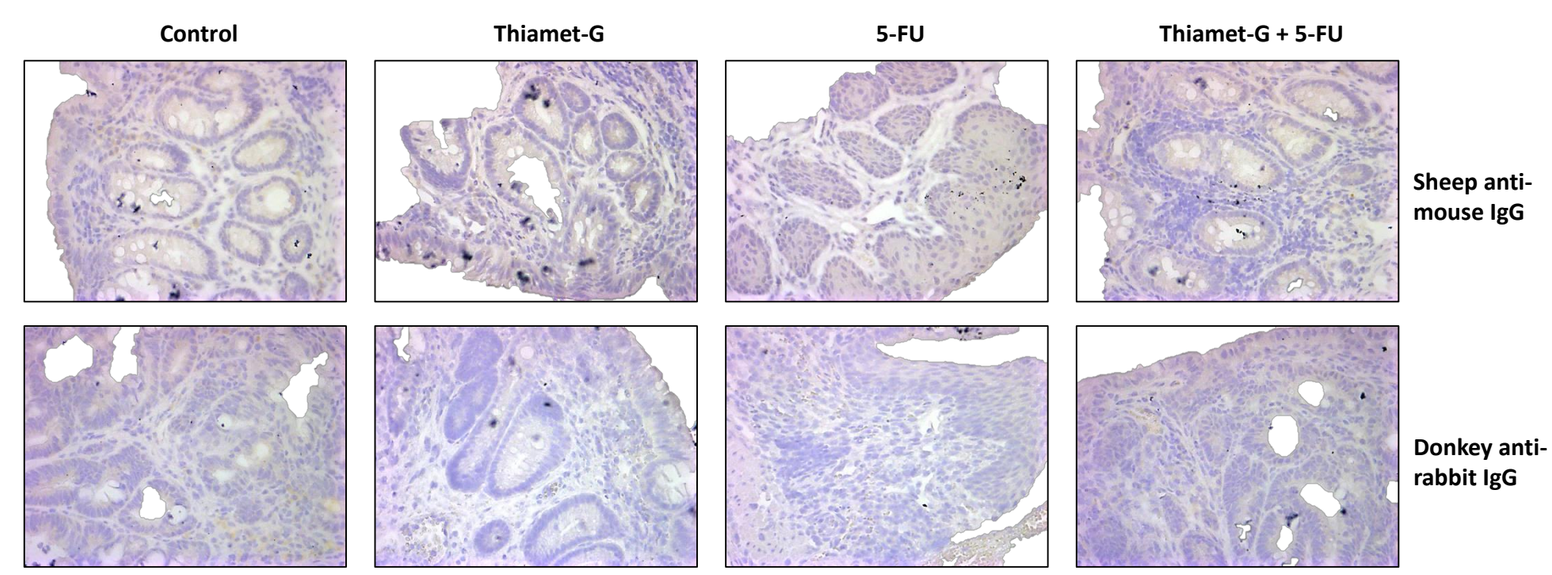

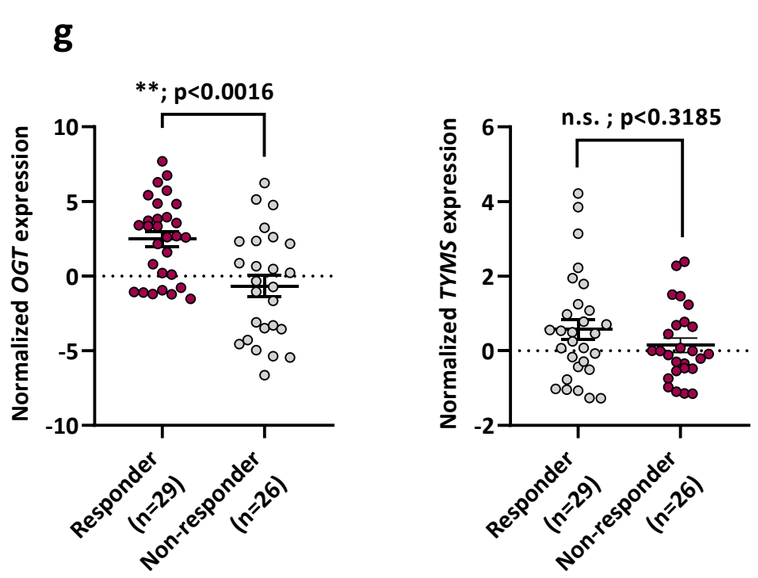

Figure 1
Very et al., 2021

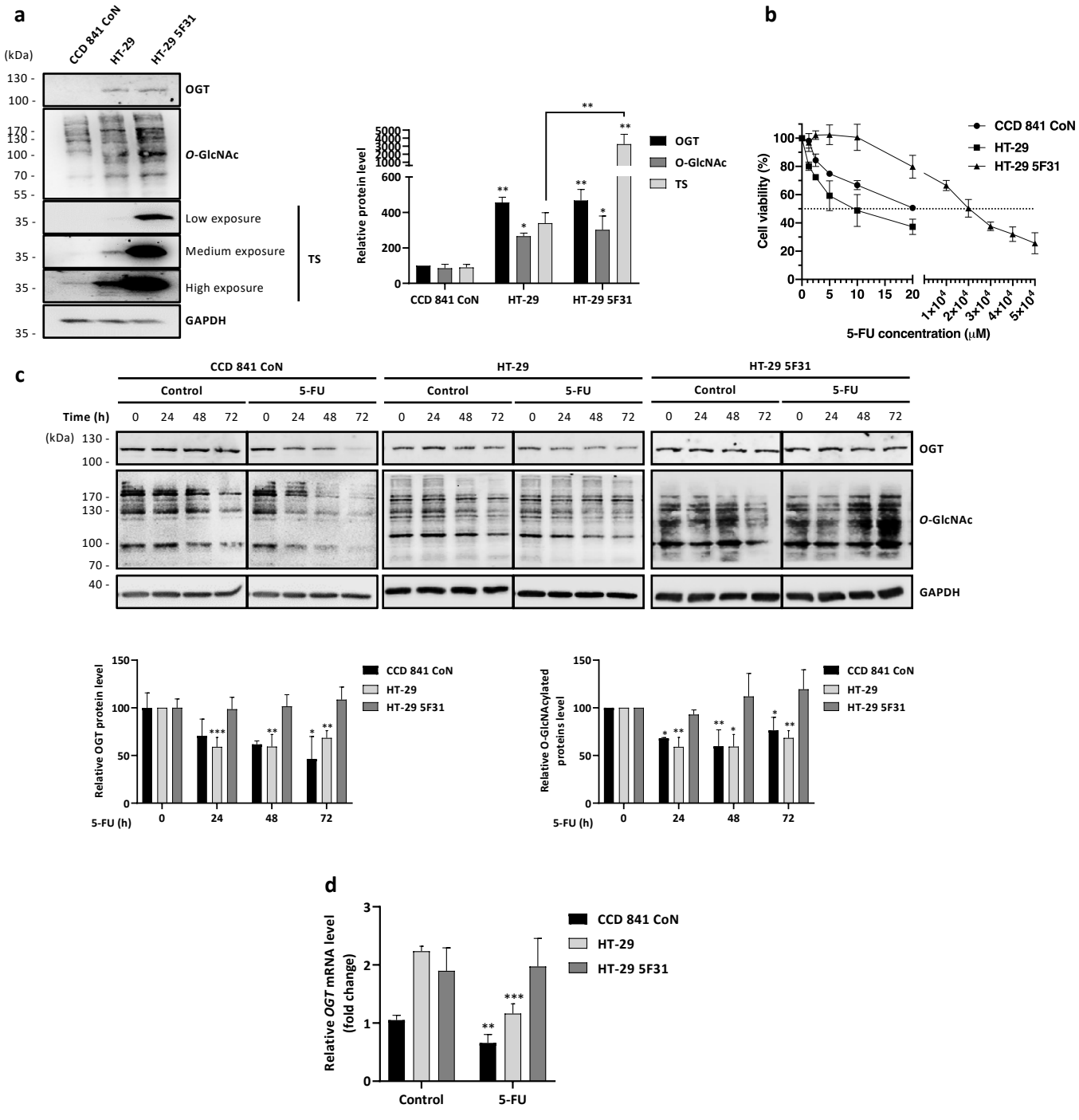

Figure 2
Very et al., 2021

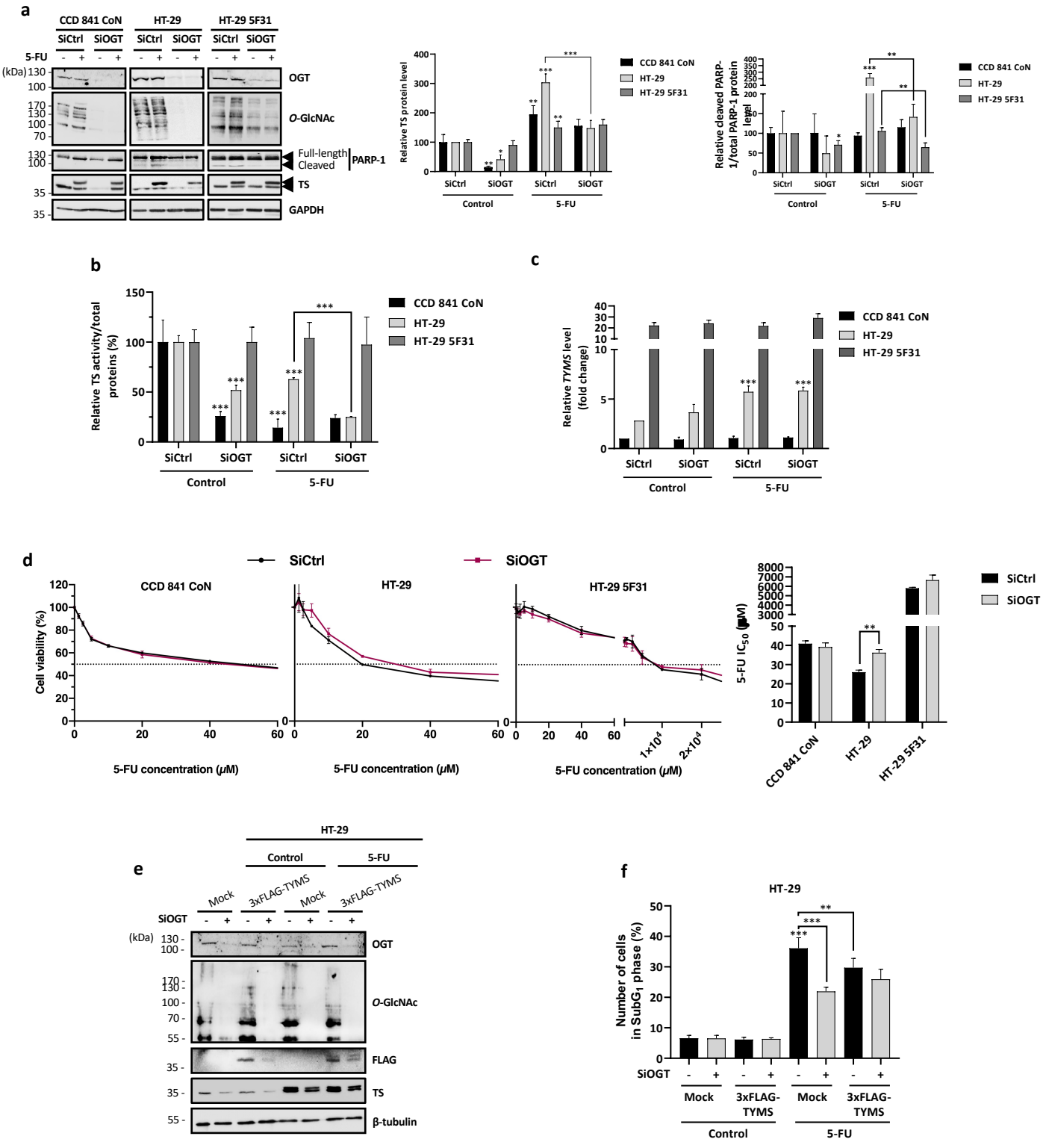

Figure 3
Very et al., 2021

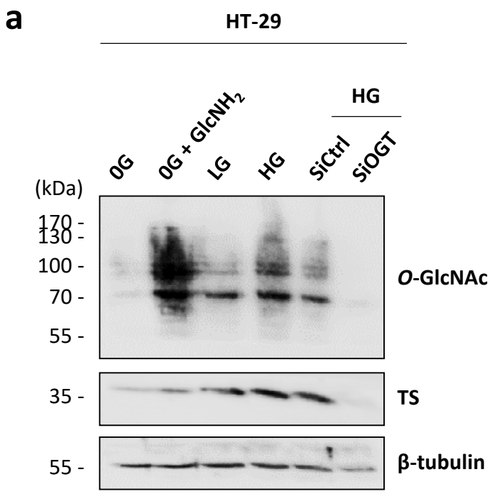

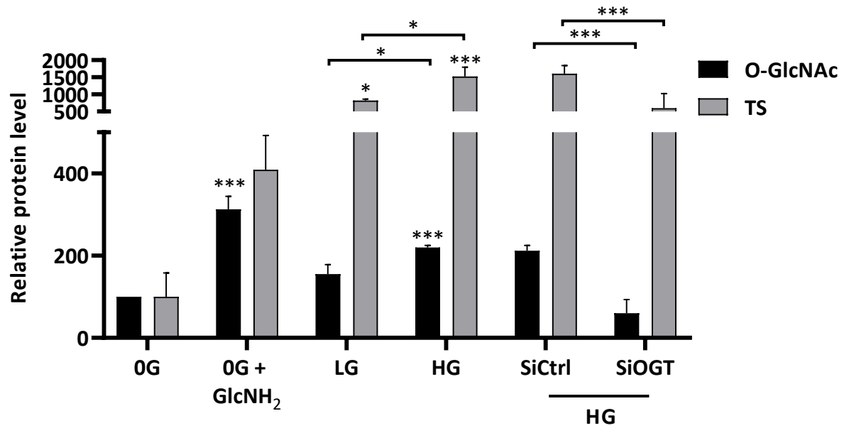

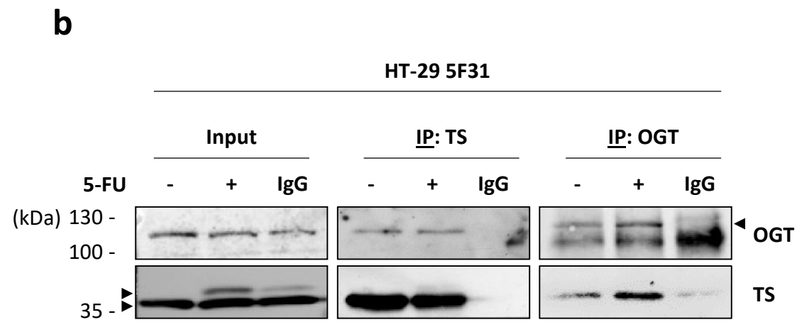

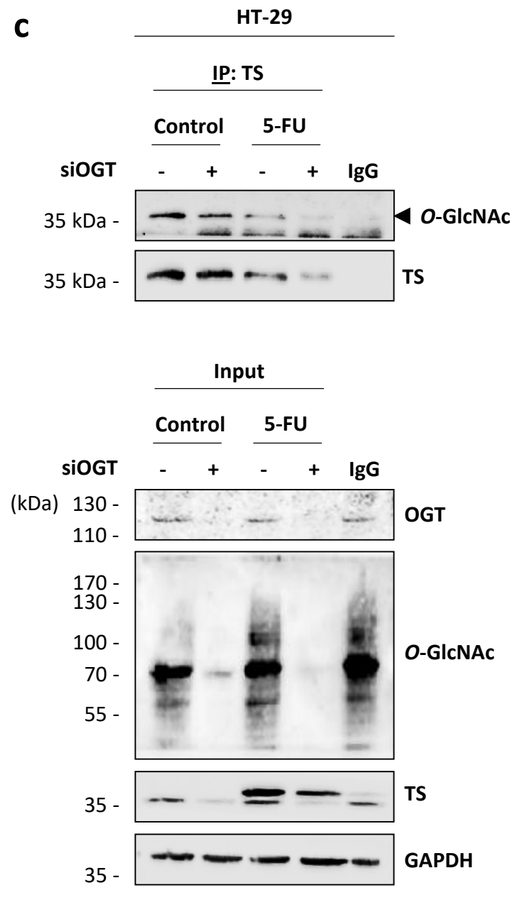

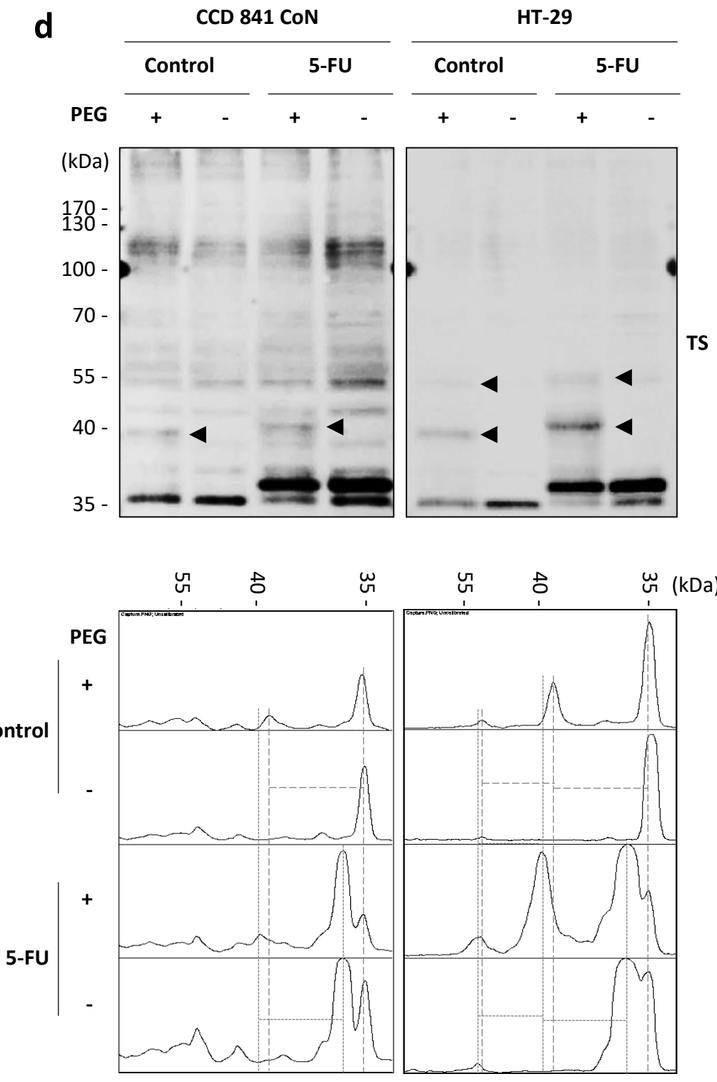

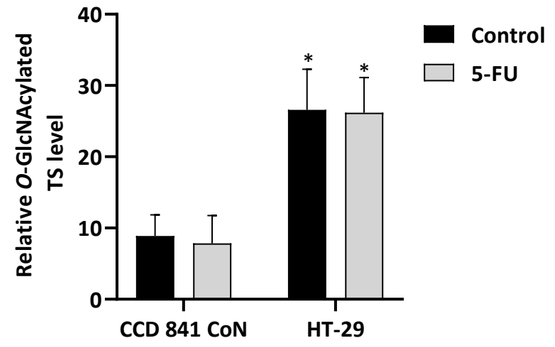

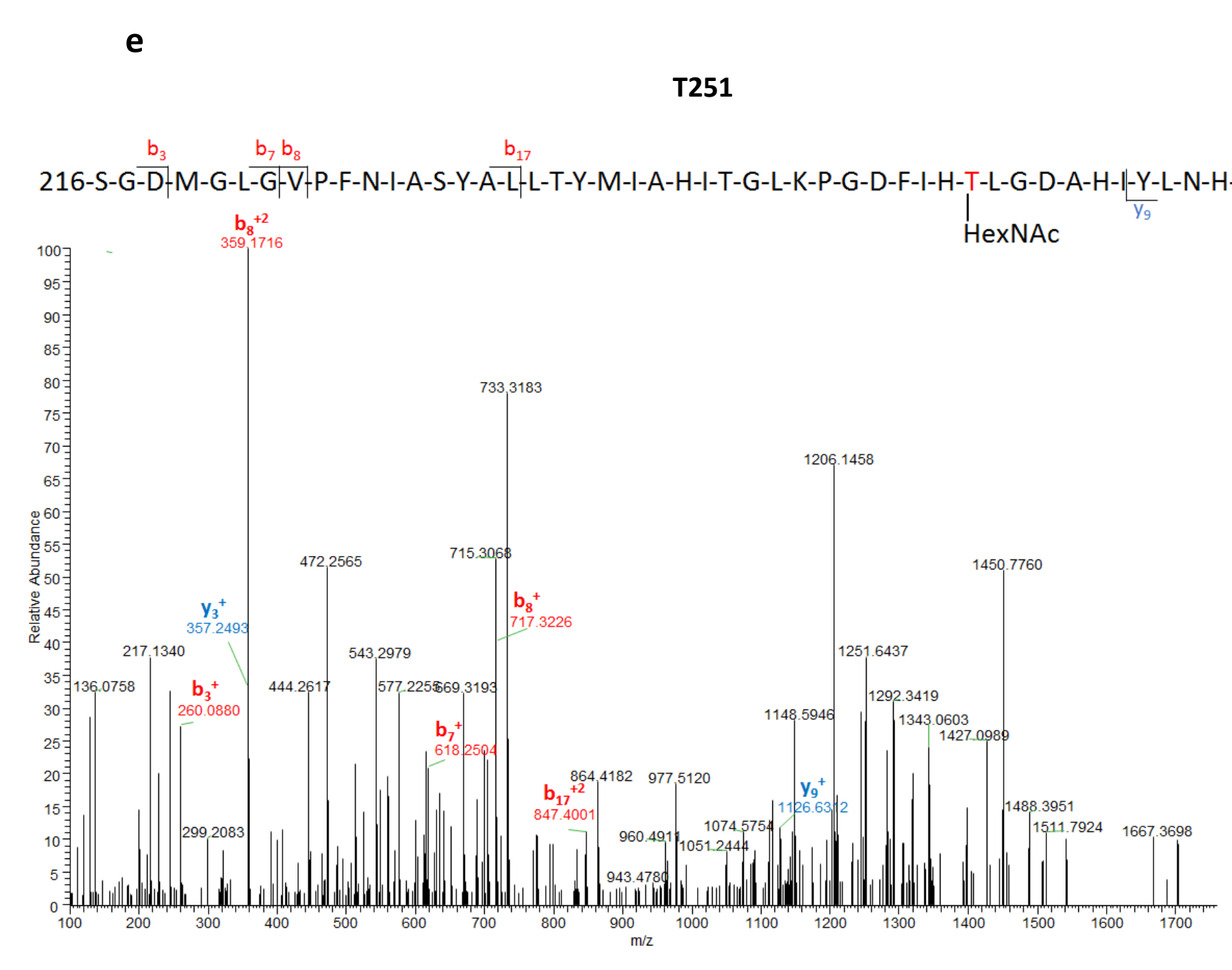

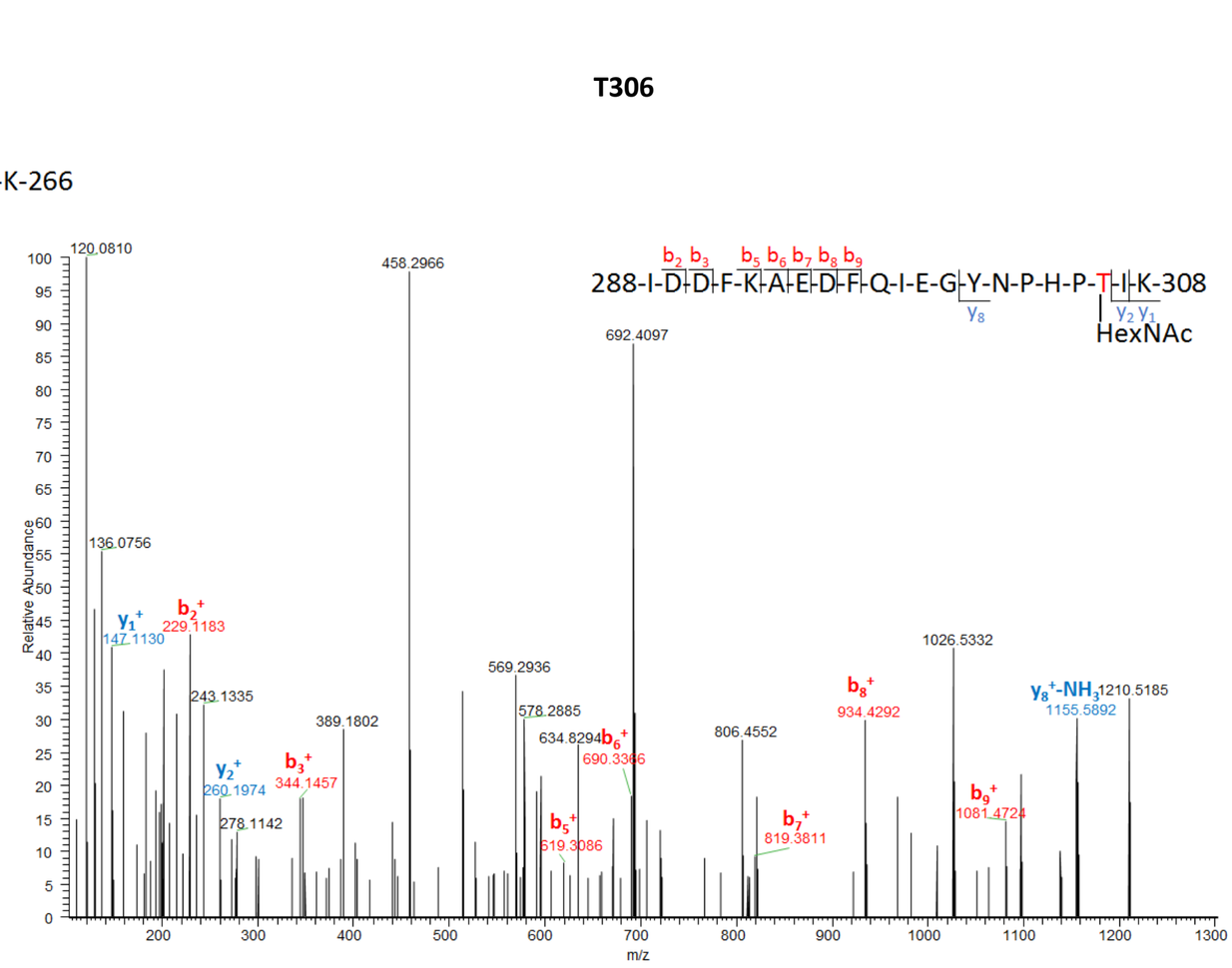

Figure 4
Very et al., 2021

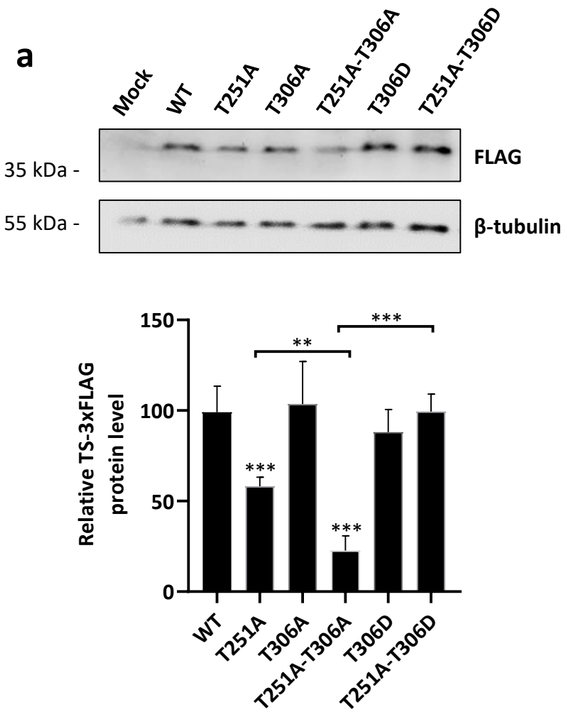

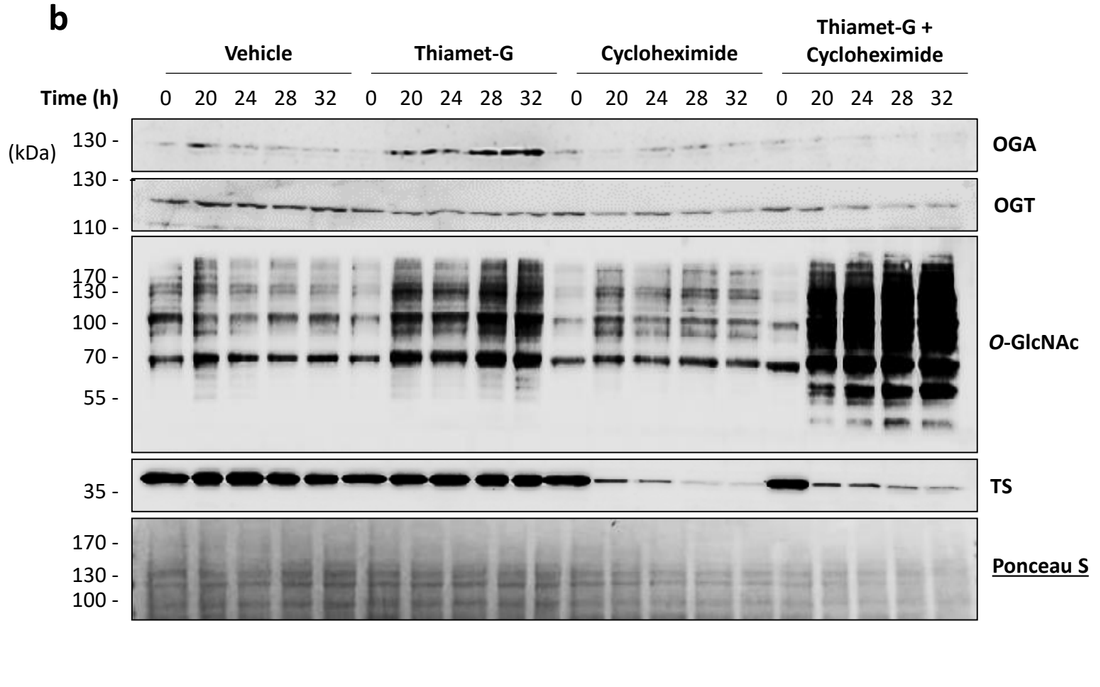

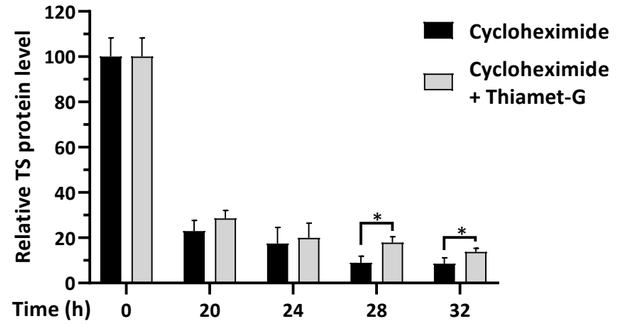

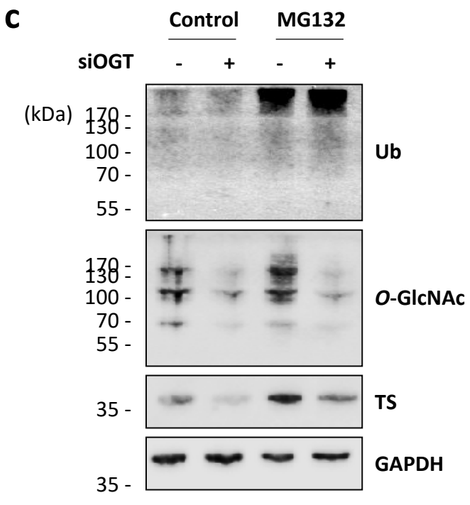

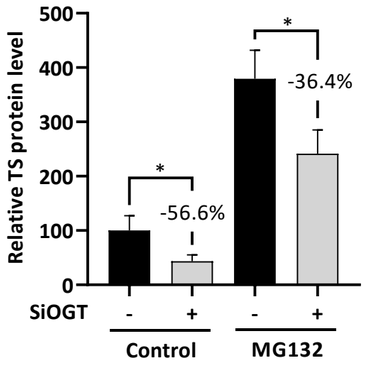

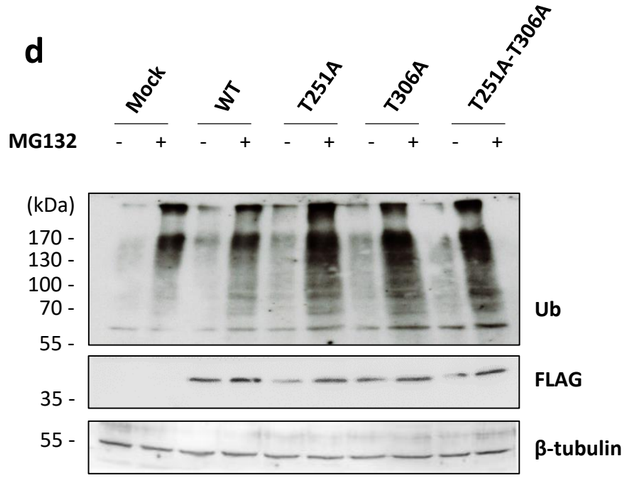

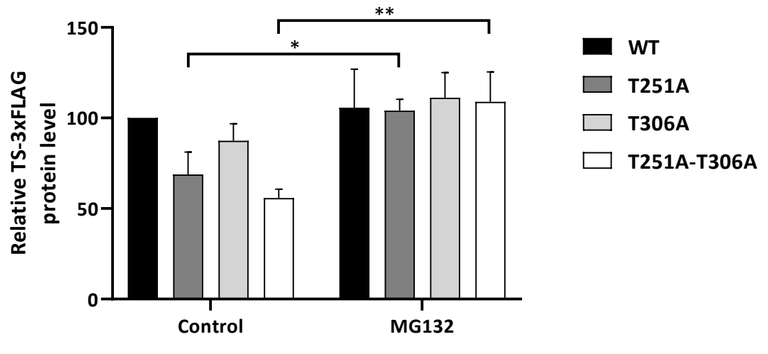

Figure 5
Very et al., 2021

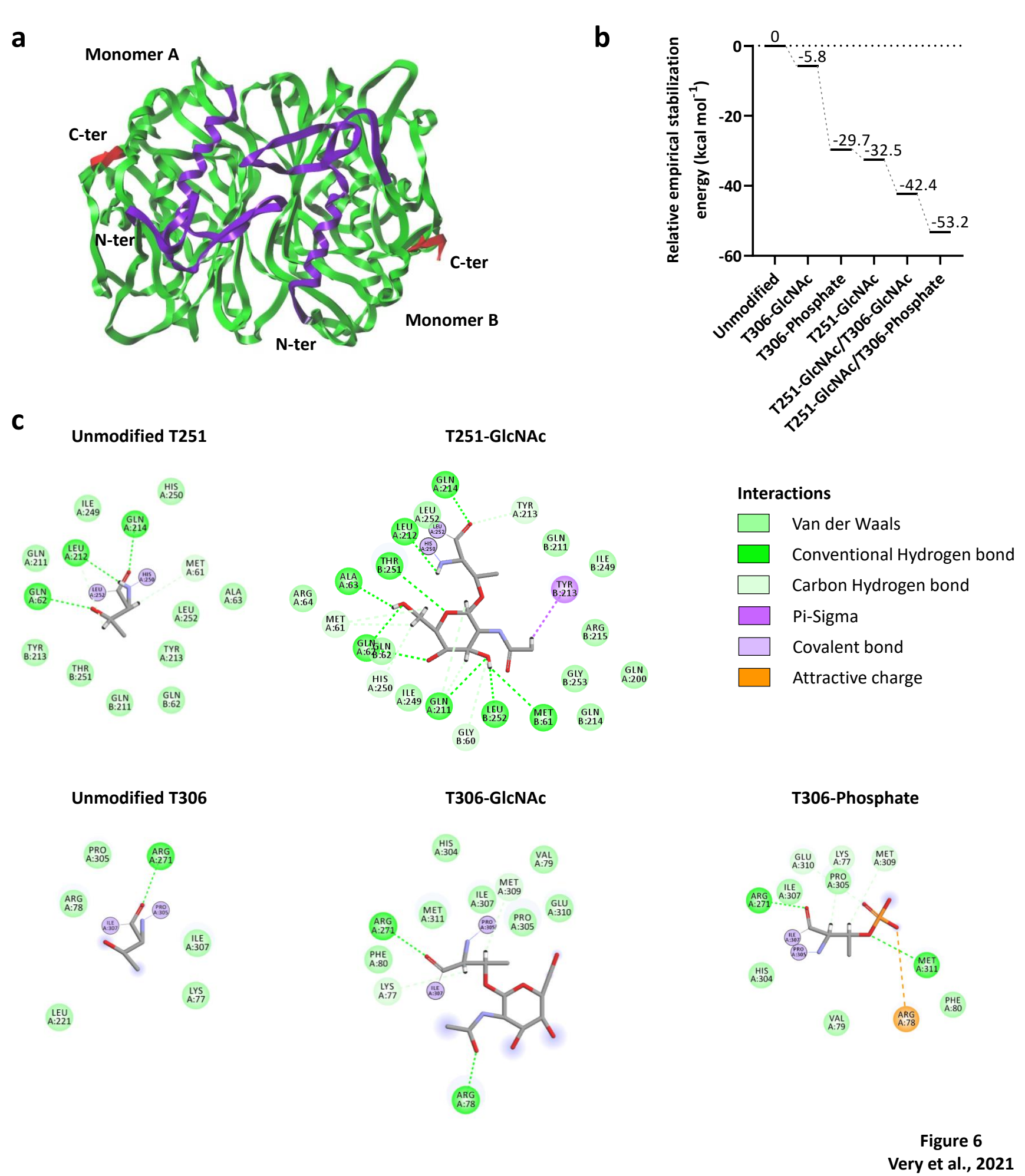

Figure 6
Very et al., 2021